HHS Public Access

Author manuscript

Nat Immunol. Author manuscript; available in PMC 2020 November 18.

Published in final edited form as:

Nat Immunol. 2020 June ; 21(6): 671–683. doi:10.1038/s41590-020-0688-3.

A Highly Polarized Th2 Bladder Response to Infection Promotes Epithelial Repair at the Expense of Preventing New Infections

Jianxuan Wu[1], **Byron W. Hayes**[2], **Cassandra Phoenix**[3], **Gustavo Sosa Macias**[4], **Yuxuan Miao**[5,6], **Hae Woong Choi**[7], **Francis M. Hughes Jr.**[8], **J. Todd Purves**[8], **R. Lee Reinhardt**[9,10], **Soman N. Abraham**[1,2,5,11,*]

[1.]Department of Immunology, Duke University Medical Center, Durham, North Carolina, USA

[2.]Department of Pathology, Duke University Medical Center, Durham, North Carolina, USA

[3.]Department of Science, North Carolina School of Science and Mathematics, Durham, North Carolina, USA

[4.]Department of Chemistry, Duke University, Durham, North Carolina, USA

[5.]Department of Molecular Genetics & Microbiology, Duke University Medical Center, Durham, North Carolina, USA

[6.]Current Address: Robin Chemers Neustein Laboratory of Mammalian Cell Biology and Development, Howard Hughes Medical Institute, The Rockefeller University, New York, New York, USA

[7.]Department of Life Sciences, Korea University, Seoul, South Korea

[8.]Department of Surgery, Division of Urology, Duke University Medical Center, Durham, North Carolina, USA

[9.]Department of Biomedical Research, National Jewish Health, Denver, Colorado, USA

[10.]Department of Immunology and Microbiology, University of Colorado Anschutz Medical Campus, Aurora, Colorado, USA

[11.]Program in Emerging Infectious Diseases, Duke-National University of Singapore, Singapore.

Abstract

Urinary tract infections (UTIs) typically evoke prompt and vigorous innate bladder immune responses including extensive exfoliation of the epithelium. To explain the basis for the extraordinarily high recurrence rates of UTIs, we examined adaptive immune responses in mouse bladders. We found that following each bladder infection, a highly T_H2 skewed immune response

* soman.abraham@duke.edu.

AUTHOR CONTRIBUTIONS

Studies were designed by J.W. and S.N.A. with help from R.L.R., T.P., M.H., and Y.M. Experiments were performed by J.W., B.H., C.P., G.S.M. and H.W.C. Data were analyzed by J.W. and S.N.A. The manuscript was written by J.W. and S.N.A. All authors contributed to discussions and manuscript review.

Competing interests

The authors declare no competing interests.

directed at bladder re-epithelization is observed with limited capacity to clear infection. Initiating this response is a distinct subset of $CD301b^{+}OX40L^{+}$ dendritic cells, which migrate into the bladder epithelium after infection before trafficking to lymph nodes to preferentially activate T_H2 cells. The bladder epithelial repair response is cumulative and aberrant, as after multiple infections, the epithelium was markedly thickened and bladder capacity was reduced relative to controls. Thus, recurrence of UTIs and associated bladder dysfunction are the outcome of the preferential focus of the adaptive immune response on epithelial repair at the expense of bacterial clearance.

Introduction

Urinary tract infections (UTIs) are common bacterial infections especially in females, where an estimated 50% of women will experience at least one UTI during their lifetime (1–5). Most UTIs are caused by uropathogenic *E.coli* (UPEC) (1–5) which typically originate from the gut (2,5). Upon reaching the bladder, these bacteria rapidly replicate in the urine and infect the bladder in large numbers. When the infection is limited to the bladder it is referred to as cystitis and when UTIs involve the kidneys pyelonephritis results (3,5,6). Noteably, UTIs have a remarkably high recurrence rate (27% to 44%) following the initial infection (3,4,7–9). For comparison, recurrence rate of pulmonary bacterial infections is around 10% (10–12), and 1.5% to 12% for gastrointestinal bacterial infections (13–15). These observations point to anomalies in the urinary immune system that predispose to infections and reinfections. Numerous animal studies have examined the innate immune responses in the bladder and kidneys to bacteria and observed powerful cytokine responses which evoked vigorous recruitment of neutrophils and monocytes (6,16–20). A characteristic bladder innate immune response is extensive shedding of the superficial epithelium which represents a powerful mechanism to reduce the load of infecting bacteria (21,22). This bladder epithelial cell (BEC) exfoliation is mediated by granule releasing mast cells found in the bladder lamina propria (LP) (22). Cumulatively, the urinary innate immune system is highly responsive in recognizing infecting bacteria and promptly clearing them through a vigorous and multifaceted immune response.

However, a unique anomaly in adaptive immune responses exists in the bladder. Whereas kidney infections evoke high levels of circulating antibodies against infecting bacteria, bladder infections evoke minimal antibodies (6,23,24,25). The bladder's inability to mount pathogen-specific antibody responses was previously used in a clincal test to differentiate cystitis from pyelonephritis (23–27). Another indication of anomalous adaptive bladder immune responses comes from the observation that a patient's history of at least two UTIs is widely considered a strong risk factor of another UTI (2–5). In view of these observations, we investigated mouse bladder adaptive immune responses following single and multiple UPEC infections. Because $CD4^{+}$ T helper (T_H) lymphocytes are the main regulators of adaptive immunity and since previous studies are not in agreement on whether CD4 T cells have any role in bacterial clearance in the bladder (28–30), we investigated the specific role of various CD4 T cell subsets (specifically T_H1 and T_H2) in promoting bacterial clearance during UTIs.

Results

The bladder T_H1 response is protective whereas the T_H2 response impedes bacteria clearance

To characterize adaptive immune responses in the bladder following infection, we focused on the roles of T_H1 and T_H2 type immune cells since a recent study suggested that T_H17 adaptive immunity is limited (31). To examine the contribution of Th1 immunity to bacterial clearance in the mouse cystitis model, we compared bacterial numbers in the bladders of wild type (WT) and T_H1 deficient *Ifng*$^{-/-}$ mice, and similarly, to study the contribution of Th2 immunity, we compared bacterial numbers in bladders of WT and T_H2 deficient *Il4*$^{-/-}$ mice. Although significant in few cases, the differences in bacterial numbers between the three groups were modest (Figure 1a). This conclusion was re-enforced when bacterial numbers in the bladder on day 21 was assessed, where no significant differences in bacterial clearance was noticed (Figure 1b). Next, we investigated if T_H1 and T_H2 mediated bladder immunity impacted secondary immune responses towards a subsequent bacterial infection. Mice were re-infected three weeks after the first infection, at a time when the numbers of persisting bacteria were very low (Figure 1b). Unlike primary responses, the *Ifng*$^{-/-}$ mice exhibited significantly impaired bacterial clearance compared to WT mice. Surprisingly, *Il4*$^{-/-}$ mice were protected as shown by bacterial clearance in their bladders being markedly more efficient than WT mice (Figure 1c). These findings suggest that whereas T_H1 cells promoted bacterial clearance, T_H2 cells, especially during the secondary response to infection, markedly impaired bacterial clearance.

A significant difference in bacterial load between WT and *Il4*$^{-/-}$ mice on Day 3 after the first infection was observed (Figure 1a). This timing is surprising because naïve CD4 T cells are typically activated after a three-day interaction with antigen presenting cells (APCs) (32–34). During bladder infection, we found a significant increase in CD4 T cell numbers on Day 3 and thereafter (Figure1d). Since rapid CD4 T cell activation is typically associated with memory cells, which secrete cytokines including IL-4 as early as 12h after activation (35–37), we wondered if the early immune responses in the bladder were linked to prior presence of memory CD4 T cells. *E. coli*-recognizing memory CD4 T cells, primed by gut microbiota (37–42), have been reported to widely exist in blood, lymphoid and non-lymphoid tissues of healthy humans and mice. Similarly, microbiota educated memory CD4 T cells may preexist in naive mouse bladders and bladder draining lymph nodes (BLNs), which are able to quickly react to bacterial infection. We pooled bladders or BLNs from 8-week-old naïve WT C57BL/6J mice and probed for memory CD4 T cells (Figure 1e). $CD44^+$ CD4 T cells are designated memory cells and CD62L further distinguishes different subtypes. We employed 8-week-old germ-free (GF) C57BL/6J mice as a negative control and 52-week-old naïve WT C57BL/6J mice, which have experienced sustained exposure to microbiota, as a positive control. We identified small and comparable numbers of CD4 T cells in the bladders of all three groups of mice, the majority of which were $CD44^+CD62L^-$ memory cells (Figure 1e). Since there was no statistical differences in bladder memory CD4 T cell numbers between WT and GF mice, the memory cells in the naïve bladder is unrelated to endogenous microbiota and they are likely self-reactive. In contrast, an almost two-fold greater number of $CD44^+CD62L^-$ memory CD4 T cells was observed in BLNs of

WT mice compared to age-matched GF mice (Figure 1e), suggesting that microbiota dependent memory CD4 T cells exist in BLN. To investigate if rapid increase of CD4 T cells in bladder following the first infection is attributable to memory cells residing in BLN, rather than in the bladder, we treated young adult mice with either vehicle control or FTY720, an agent which inhibits T cell migration from lymph nodes to non-lymphoid tissues (43). On Day 3 post infection, FTY720 treated mice failed to exhibit an increase in CD4 T cells (Figure 1f). Thus, the unexpectedly early CD4 T cell response to the first UPEC infection is attributable to preexistence of memory CD4 T cells in BLNs, which presumably are primed by endogenous microflora.

The bladder response to a subsequent infection is highly T_H2 biased.

To understand bladder T_H1 and T_H2 cell responses to re-infection, we assessed their dynamics in IFN-γ reporter mice (Great) and IL-4 reporter mice (4get). The IFNγ reporter mice were created by tagging an internal ribosomal entry site (IRES)-yellow fluorescent protein (YFP) cassette at the 3' end of the endogenous *Ifng* gene (44,45), while the IL-4 reporter mice were created by tagging an IRES-enhanced green fluorescent protein (GFP) at the 3' end of endogenous *Il4* gene (44,46). We examined the dynamics of IFN-γ^+ CD4 T cells (T_H1) and IL-4^+ CD4 T cells (T_H2) in these reporter mice following a first and second pyelonephritis infection (Supplement figure 1a), in which both bladder and kidneys are infected. The kidney is used as control organ, as its adaptive immune responses following UTIs are known to be unimpaired and effective (6,16,20,28). In the first three days following initial infection, there was a lower percentage of IFN-γ^+ CD4 T cells in bladder compared to the kidney (Figure 2a). However, by Day 7 the bladder and kidney showed a similar percentage of IFNγ^+ CD4 T cells probably because kidneys clear bacterial rapidly (6,47). In contrast, when examining for IL-4^+ CD4 T cells after initial infection, we found that the bladder contained a higher percentage of IL-4^+ CD4 T cells compared to kidneys (Figure 2b). Consistent with these data, IL-4^+ CD4 T cell numbers, presented as a percentage of total live single cells in the bladder, were higher than IFN-γ^+ CD4 T cell numbers on day 3 post-infection (Supplement figure 1d). When we examined reporter mice after 2nd bacterial infection, the bladder exhibited a further increase in percentage of IL-4^+ CD4 T cells but not IFN-γ^+ CD4 T cells (Figure 2c, 2d, Supplement figure 1e). Thus, in contrast to the kidneys which exhibit a balanced immune response, the bladders exhibit a strong Th2 bias following infection.

Next, we sought to confirm the bladder T_H2 bias in mice experiencing only cystitis. We induced cystitis (as in Figure 1) in Great and 4get mice and found a similar T_H2 bias after the first infection which was enhanced after a second infection (Supplement figure 2a, 2b). We also examined if a T_H2 bias was observed in two different WT strains (C57BL/6J and BALB/cJ). We assessed IFN-γ and IL-4 cytokine production by ELISA after the 1st and 2nd cystitis infections. We found that the T_H2 bias (higher IL-4 production compared to IFN-γ) in the bladders of C57BL/6J was not evident in the first infection but was clear after a subsequent infection. In BALB/cJ mice, we found the Th2 bias was evident after both the 1st and 2nd infection (Figure 2e, 2f). To support our contention of Th2 bias, we directly visualized and quantified T_H1 and T_H2 cells in WT C57BL/6J mouse bladders (Supplement figure 2c). We found that there were more GATA3$^+$CD4$^+$ T_H2 cells than T-bet$^+$CD4$^+$ T_H1

cells in infected mouse bladders (Supplement figure 2d). These data confirm bladder Th2 bias in both pyelonephritis and cystitis-only models, which is further increased after a secondary infection.

T_H2 biased immune response to infection in the bladder is directed at epithelial repair

Since the Th2 biased immune response had limited capacity to clear bacteria, we reasoned that it had another physiologic purpose. Studies examining T_H2-mediated immune responses during parasitic infections have pointed to two major roles. One is to recruite mast cells and eosinophils which directly clear the parasite (48,49), and the other is to stimulate growth factor secretion from surrounding cells to induce epithelial cell proliferation (48,50,51). This latter activity is necessary to restore the epithelial barrier destroyed by the invading parasite (48). In view of the powerful bladder innate immune responses to infection resulting in extensive exfoliation of the epithelium and subsequent exposure of underlying tissue to noxious ammonia and salts in urine (22), we hypothesized a key response of the adaptive immune response is restoring the bladder epithelium.

To test this notion, we compared epithelial recovery following infection in WT and *Il4*$^{-/-}$ mice. We examined the epithelial surfaces of both groups of mice using wheat germ agglutinin (WGA)-FITC as a probe (22) on Day 0, 1 and 3 after infection to assess for epithelial regeneration. In both mice, the superficial epithelium was lost by Day 1 post-infection. By Day 3, appreciable superficial epithelium regeneration was evident in WT, but not in *Il4*$^{-/-}$ mice (Figure 3a). We also intravesically inoculated dextran conjugated with Texas Red, which only penetrates damaged bladder epithelium (Figure 3b). Strong dextran penetration was observed in both WT mice and *Il4*$^{-/-}$ mice on Day 1 post-infection. On Day 3, we observed limited penetrance of dextran into the bladder tissue in WT mice, compared to *Il4*$^{-/-}$ mice (Figure 3b). Epithelial recovery can also be assessed by examining barrier function following administration of trypan blue dye. We observed similar results with trypan blue assay (Figure 3c).

To see if differences in bladder permeability was specifically related to T_H2 cell deficiency in *Il4*$^{-/-}$ mice, CD4 T cells derived from the BLNs of twice-infected 4get mice were differentiated *in vitro* under either T_H2 condition or T_H0 condition (supplement figure 3a, 3b) and adoptively infused into *Il4*$^{-/-}$ mice. We found that the *Il4*$^{-/-}$ mice receiving T_H2 cells exhibited comparable bladder epithelial recovery to WT mice (Figure 3d) whereas *Il4*$^{-/-}$ mice receiving T_H0 cells exhibited the same defective phenotype exhibited by *Il4*$^{-/-}$ mice not subjected to adoptive transfer (Figure 3d). These results confirm that Th2 cells are essential in restoring the bladder barrier after UPEC infection.

We showed that activated T cells responding to bladder infection originated from BLNs (Figure 1f). If the superficial BEC regeneration is mediated by activated T cells from BLNs, inhibiting their migration into the bladder should inhibit the epithelial regeneration. This was observed during bladder infection (Figure 3e). Our data suggested CD4 T cells from BLNs reacted rapidly to UPEC as memory cells (Figure 1). We questioned if the observed superficial BEC recovery following infection was bacterial antigen-specific. We sorted IL-4 GFP$^+$ cells from twice infected 4get mice and then adoptively transferred them into *Il4*$^{-/-}$ mice. As control T_H2 group, we *in vitro* stimulated non-specific naïve CD4 T cells under

T_H2 culture condition (Supplement figure 3c) before adoptive transfer into *Il4*$^{-/-}$ mice. After infection, WT and *Il4*$^{-/-}$ mice harboring bacterial antigen-specific T_H2 cells exhibited good and comparable superficial BEC recovery whereas *Il4*$^{-/-}$ mice and *Il4*$^{-/-}$ mice infused with control T_H2 cells exhibited defective epithelial recovery (Figure 3f, Supplement figure 3d). Thus, T_H2 cells are activated in an antigen-dependent manner to mediate epithelium repair.

If exfoliation is the original cause for Th2 bias, predictably, this response should be absent in bladders that fail to exfoliate during infection. Bladders of chymase deficient (*Mcpt4*$^{-/-}$) mice exhibit markedly less exfoliation following infection compared to WT mice (22). Compared to *Mcpt4*$^{+/+}$ 4get mice, we found that the T_H2 response was significantly weakened in the *Mcpt4*$^{-/-}$ 4get mice (Figure 3g). Conversely, the T_H1 response was enhanced in the exfoliation-deficient mice (Figure 3h). Thus, the Th2 bias is a specific response to bladder exfoliation.

Next, we explored the mechanism of Th2-mediated bladder superficial epithelial regeneration. Since IL-4 regulates several growth factors (48–51), we examined their expression in bladder following infection by RT-PCR. Three of five growth factors tested, EGF, TGFα and IGF-1, were upregulated in bladder from day 0 to day 3 after infection (Figure 4a). All three factors increased uptake of BrdU in a dosage-dependent manner in *in vitro* culture, suggesting they promote BEC proliferation (Figure 4b, 4c, 4d). We also compared expression levels in infected bladders of WT, *Il4*$^{-/-}$ and *Il4*$^{-/-}$ mice infused with T_H2 cells. Our results indicate expression of these growth factors was significantly decreased in *Il4*$^{-/-}$ mice compared to WT or *Il4*$^{-/-}$ mice infused with T_H2 cells (Figure 4e). Thus, EGF, TGFα and IGF-1 production is stimulated by T_H2 cells to promote epithelial regeneration during bladder infection.

Since M2 macrophages promote IL-4-mediated growth factor secretion (48–51), we examined if bladder expression of EGF, TGFα and IGF-1 correlated with the presence of M2 macrophages. The expression level of M2 macrophage signature genes (50,52,53) in bladder tissue was significantly reduced in *Il4*$^{-/-}$ mice compared to their level in WT mice and in *Il4*$^{-/-}$ mice infused with T_H2 cells (Figure 4f). These results were confirmed by flow cytometry (Supplement figure 4a, 4b). Thus, M2 macrophages also contribute to IL-4-regulated immune responses in bladder infection. Furthermore, applying M2 macrophage inhibitor GW2580 (54–56) can significantly reduce the concentration of growth factors in bladder lysate and inhibit epithelial repair (Figure 4g, Supplement figure 4c, 4d) while not affecting Th2 cells (Supplement figure 4e). Therefore, M2 macrophage function downstream of IL-4, and directly or indirectly stimulate growth factor production during bladder infections.

CD301b$^+$ DCs direct T_H2 bias in the bladder

Since activation and recruitment of CD4 T cells is mediated by APCs, we sought to identify the particular APCs involved in bladder. A dendritic cell (DC) subset, CD301b$^+$CD11c$^+$, mostly described in the skin, was shown to drive T_H2 responses following parasitic infections (57–60). Therefore, we infected the bladders of WT mice with UPEC J96 and stained for CD301b 12 h after infection. An appreciable number of CD301b$^+$ cells were resident in the LP region of control bladders (Figure 5a). Interestingly, by 12 hours after

UPEC infection, a proportion of these cells had migrated into the epithelium (Figure 5a). Thus, CD301b$^+$ cells are present in the bladder and have the potential to directly sample antigens in the epithelium. To confirm this, the bladders, BLNs, and the kidney-draining renal lymph nodes (KLN) were collected and analysed on day 0 and day 1 after infection (Supplement figure 5a, 5b). We observed that a significant proportion of MHC class II$^+$ APCs in bladder were CD11c$^+$CD301b$^+$ DCs on day 0 (Figure 5b). On Day 1 post infection, the percentage of these cells significantly decreased in the bladder (Figure 5b). This decrease corresponded with a large increase in CD301b$^+$CD11c$^+$ DCs in BLN (Figure 5b). That was not seen in the KLN. The chemokine receptors CCR7 and CCR8 are important for CD301b$^+$ DCs migration from the skin to draining lymph nodes (61). Flow cytometry analysis revealed that CCR7, but not CCR8, is highly expressed on bladder CD301b$^+$CD11c$^+$ DCs at 12 h and thereafter post infection, and nearly all of CD301b$^+$CD11c$^+$ DCs that had migrated into BLNs expressed CCR7 (Supplement figure 5c, 5d). Their migration into BLN was also confirmed by microscopy (Supplement figure 6). These results indicate that CD301b$^+$CD11c$^+$ DCs reside in bladder LP in the steady state, but following infection, they migrate to BLN to activate CD4 T cells.

To demonstrate the ability of DCs to initiate the activation and migration of T_H2 cells into the bladder following infection, we bred CD301b^{DTR} mice with 4get or Great mice, to generate CD301b^{DTR} mice with IL-4 reporter capacity and CD301b^{DTR} mice with IFN-γ reporter capacity. We then treated half of these mice with diphtheria toxin (DT), and the other half with PBS as a control. As additional control for DT treatment, we treated WT 4get mice with DT. In contrast to CD301b^{DTR} mice treated with PBS and WT 4get mice treated with DT, CD301b^{DTR} mice treated with DT harbored minimal amounts of IL-4$^+$ CD4 T cells in bladder infection (Figure 5c), suggesting CD301b$^+$ cells were activating Th2 cells. We confirmed this after a second infection (Figure 5d). Interestingly, when we examined IFN-γ reporter mice, we found depletion of CD301b$^+$ cells caused a significant increase of IFN-γ$^+$ CD4 T cells (Figure 5e). Similar results were observed after a second infection (Figure 5f). Furthermore, the bladder epithelium regeneration in mice depleted in CD301b$^+$ cells was significantly impaired compared to WT mice (Figure 5g). Meanwhile, we found a significantly lower CFU in CD301b$^+$-depleted mice compared to WT mice after a second infection (Figure 5h), confirming role of CD301b$^+$ cells in promoting T_H2 bias which impedes bladder bacterial clearance.

OX40L on CD301b$^+$ DCs is responsible for the T_H2 bias in bladder.

Next, we investigated how CD301b$^+$ DCs induced bladder Th2 bias. The nature and expression levels of co-stimulatory ligands on surface of APCs are critical in guiding T_H1- and T_H2- polarization (48,49,57,62,63). Whereas OX40L, PD-L2, ICOSL, and JAG1 are ligands that induce T_H2 responses (48,49,57), DLL1 and DLL4 are ligands that induce T_H1 responses (62,63). CD301b$^+$ DCs found in the skin constitutively express high levels of PD-L2 and low levels of OX40L (57,60), and no Th1-inducing ligands have as yet been reported on these cells (57,60). To examine if a similar molecular expression pattern of co-stimulatory ligands was occurring on bladder CD301b$^+$ DCs, we assessed expression of those ligands on bladder APCs (7AAD$^-$CD45$^+$MHC class II$^+$) at 0h, 12h and 24h after infection by flow cytometry. We grouped the APCs into three subpopulations:,CD301b

$^{+}$CD11c^{+} cells (CD301b^{+} DCs), CD301b^{-}CD11c^{+} cells (other DCs and APCs), CD301b^{-}CD11c^{-} cells (B cells, macrophages and other APCs) (Figure 6a). We found that at 0h approximately 40% of CD301b^{+}CD11c^{+} cells expressed the T_H2 inducing ligand OX40L (OX40L^{+}PD-L2^{-}). However, none of the other subpopulations expressed other Type 1 or 2 ligands (Figure 6a). 12 hours post-infection, a proportion of the CD301b^{+}CD11c^{+} and the CD301b^{-}CD11c^{+} populations expressed high amounts of PD-L2 (OX40L^{low}PD-L2^{+}) and intermediate levels of ICOSL. Notably, OX40L^{+}PD-L2^{-} and OX40L^{low}PD-L2^{+} are two distinct populations among CD301b^{+}CD11c^{+} cells. This observation differs from the skin, where only one T_H2-driving population OX40L^{lo}PD-L2+ cells exists. In contrast to OX40L^{low}PD-L2^{+} population of CD301b^{+} DCs, by 24 hours following infection, the percentage of bladder-specific OX40L^{+}PD-L2^{-} cells decreases sharply, presumably because of their migration to BLNs. Importantly, none of the bladder APCs expressed noticeable DLL1/4 ligands (Figure 6a). Thus, OX40L is the only ligand constitutvely and exclusively expressed on bladder CD301b^{+} DCs.

Since PD-L2 and ICOSL are also expressed on bladder APCs, it is important to rule out their contribution to T_H2 responses. To investigate their function, we intraperitoneally infused anti-OX40L antibody (Ab), anti-PD-L2 Ab, anti-ICOSL Ab or isotype control Ab into 4get or Great mice. We then collected the bladders three days after infection for flow cytometry analysis and found that anti-OX40L Ab caused a significant decrease of T_H2 cells compared to the control group (Figure 6b), whereas anti-PD-L2 and anti-ICOSL had no significant effect (Figure 6b). These results point to the importance of OX40L. We also examined OX40L^{+}CD301b^{+} DCs by microscopy and found that almost all of the CD301b^{+} DCs that migrated into the epithelium by 12h post infection were OX40L^{+} (Figure 6c). These observations point to OX40L on CD301b^{+} DCs as a critical determinant of T_H2 responses in the bladder following UPEC infection.

Th2 biased immune responses to repeated infections is detrimental to bladder function in multiple ways.

As T_H1 and T_H2 cells mutually inhibit each other (64–66), the strong T_H2 environment in a multiple-infected bladder will predictably overcome any residual T_H1 responses that it is capable of mounting. To investigate this, we bred *Il4*$^{-/-}$ mice with Great mice to create IFN-γ reporter mice with a T_H2 deficiency. Examination of the percentage of IFN-γ^{+} CD4 T cells in *Il4*$^{-/-}$ and *Il4*$^{+/-}$ mice showed a significant increase in these cells compared to *Il4*$^{+/+}$ mice (Figure 7a). Thus, T_H2 cells in the bladder have the capacity to reduce the number and bacterial clearance capacity of T_H1 cells in this organ. Furthermore, when large numbers of UPEC-specific T_H1 cells were adoptively infused into *Ifng*$^{-/-}$ mice, the bladder's bacterial clearing capacity was rescued, indicating that although T_H1 cells are intrinsically capable of clearing bacteria this ability is inhibited in WT mice by the presence of T_H2 cells (Supplement figure 7).

In view of enhanced T_H2 biased responses following a subsequent bladder infections, we investigated if there are any noticeable effects of repeated infections on bladder architecture. We infected mice one, two or three times with UPEC J96 and then examined bladder sections for morphological changes on day 3 after the final infection (Figure 7b). Bladders

of control mice exposed to PBS exhibited an intact epithelium (Figure 7b) while bladders of mice challenged with a single infection appeared to only partially recover their superficial epithelium (Figure 7b). Bladders of mice that experienced two infections had completely recovered their superficial epithelium (Figure 7b). Mice that experienced three infections had acquired a significantly thicker epithelium pointing to the existence of an enhanced epithelial cell proliferation program (Figure 7b). Seemingly, the capacity to regenerate the epithelium appears to accelerate and grow with each infectious bout (Figure 7b). When we compared bladder functions of three-time infected mice with control mice, we observed significant loss of bladder capacity which is defined as urine retention ability in infected mice compared to control mice, as the former tended to void urine much more frequently than the control (Figure 7c). The rapid T_H2-initiated tissue repair program appears suboptimal as multi-re-epithelized bladders exhibit diminished capacity to store urine. Thus, bladders of multiple-infected mice are not only compromised in their capacity to clear infections, but they are also functionally limited. Finally, we questoned if these defects were temporary or more long lasting. We investigated bladder epithelial architecture, bladder T_H2 cell numbers and bladder capacity in three-time-infected mice two months after the last infection (Figure 7d–f). Although aberrant bladder epithelial remodeling is long-lasting, there appears marked individual variation.

Discussion

Our goal was to identify unique aspects of the bladder's adaptive immune response that predispose to re-infection. We report that following bacterial infection, the bladder evokes a vigorous T cell response with a distinct T_H2 bias which is further enhanced during subsequent infections. The T_H2 directed immune response focuses on repairing the superficial bladder epithelium following infection-triggered exfoliation of this barrier. This enhanced bladder Th2 response also paralleled a corresponding decrease in bacteria-clearing T_H1 responses. This epithelial repair mechanism could be unique to the bladder as extensive exfoliation of the epithelium is not typically observed at mucosal sites. The prominent role played by bladder T cells in mediating epithelial repair activities was previously unknown because T cell numbers in the bladder are small and difficult to isolate and study. We overcame this technical difficulty by using recently created IFN-γ and IL-4 reporter mice which markedly enhanced our ability to detect both T_H1 and T_H2 cells.

Although a T_H2 biased response has previously been implicated in parasite clearance (48,49), this is the first time such a response has been reported for bacterial infections, albeit with limited bacterial clearance capabilities. The speed and vigor of the T_H2-mediated epithelial regeneration process appears to increase with each infection. Conceivably, urgent repair of the bladder epithelium is needed following bacteria-induced epithelial exfoliation. Any delay in repair will prolong the time the underlying tissue is exposed to urine which is replete with cytotoxic and pain-inducing salts and noxious compounds. Even though limited bacterial clearance predisposes to another infection, it could represent the lesser of two evils.

Rapid epithelial repair activity was observed even following a primary infection and involved memory T_H2 cells educated by the endogenous microbiota. The existence of microbiota in the healthy human bladder was recently reported (67,68). This overarching

focus on bladder epithelium repair also appears to be why the bladder fails to mount an antibody response to infecting UPEC (6). Following infection-induced loss of the bladder epithelium, bladder mast cells spontaneously secrete large amounts of the immunosuppressive cytokine, IL-10, to subdue local inflammation so that epithelial repair can occur (6). An unintended consequence of this action is inactivation of bladder DCs resulting in limited antibody responses to infecting bacteria (6).

That bladders exposed to consecutive infections exhibited markedly thickened epithelia and reduced bladder capacity has not previously been reported, but is consistent with current views that repeated UTIs may cause lasting changes in bladder function (69,70). This finding and that at least 50% of interstitial cystitis patients experiencing bladder disorders (e.g. nocturia) have a prior history of recurrent UTIs (1–5), suggest that patients experiencing recurrent UTIs should be examined for changes in bladder functions.

We have discovered a critical role for CD301b$^+$ DCs in directing T_H2 biased responses in the bladder. These cells that are resident in the LP of the bladder migrated into the epithelium during infection and then trafficked to the draining lymph nodes where they triggered the mobilization of T_H2 T cells into the bladder. We showed that OX40L on CD301b$^+$ DCs is responsible for inducing the T_H2 response. Although CD301b$^+$ DCs, which are PDL2$^+$OX40L^{lo}, have previously been implicated in the T_H2 responses to parasitic skin infections (57,60), only a subset of bladder CD301b$^+$ DCs, namely PDL2$^-$ OX40L$^+$, were implicated in T_H2 responses during bacterial infection. Indeed, neutralization of OX40L in the bladder significantly mitigated the T_H2 bias following bacterial infection, which is in contrast to findings in parasite skin infections where these anti-OX40L antibodies had no effect (60). As OX40L is a different T_H2 ligand expressed by bladder CD301b$^+$ cells compared to skin CD301b$^+$ cells (57,60), T_H2 inducing mechanisms by CD301b$^+$ DCs may differ based on the unique local microenvironment. Why OX40L is constitutively expressed on bladder CD301b$^+$ DCs is currently unknown, but it is noteworthy that these DCs are specifically recruited into the uroepithelium where they encounter infecting bacteria. During bladder infections, mast cells migrate into the epithelium to mediate exfoliation of the superficial epithelium (22). Concurrent with this activity, mast cells presumably secrete chemoattractants and cytokines such as IL-13 promoting the recruitment of CD301b$^+$OX40L$^+$ DCs into the epithelium as has been previously suggested for allergen-induced airway inflammation (71,72).

Even though a patient's history of previous UTIs is generally considered a strong risk factor for another UTI (1–5), the underlying basis has until now remained elusive. This is probably because previous studies have largely overlooked the contributions of immune responses following repeated infections (28–30). Moreover, few studies have focused on the adaptive immune response which appears to be a major player following repeated bacterial infections. Recently, it was suggested that "mucosal imprints" left by prior *E. coli* bladder infection, especially after chronic infections, can markedly sensitize bladders to recurrent disease (73,74). Along these lines, we have found that bladder infections trigger a T_H2 biased response impacting both the bladder structure and function and that the magnitude of these responses increase with each infection. Since these T_H2 enhanced responses proportionally inhibit T_H1 mediated responses, especially its bacteria-clearing activities, the result leads to

reinfections. This finding of an aberrant bladder immune response to infection raises the possibility of employing immune modulatory strategies to combat UTIs.

METHODS

Mice

Female C57BL/6J mice were purchased from the Jackson Laboratory and housed in animal facility of Duke University till experiments were performed. *Ifng*$^{-/-}$ (002287), *Il4*$^{-/-}$ (002253), CD301b^{DTR} (023822) mice were obtained from the Jackson Laboratory and bred in animal facility of Duke University. IL-4 reporter mice (4get) and IFN-γ reporter mice (Great) were graciously provided by Richard Locksley (University of California, San Francisco) and were bred to C57BL/6J mice for more than ten generations. All of the above mice were housed under specific pathogen free (SPF) condition in animal facility of Duke University and eight- to ten-week old mice were used for all the experiments unless otherwise noted. 8-week-old germ-free C57BL/6J mice were purchased from the animal facility of Duke Division of Laboratory Animal Resources (DLAR). All mouse experiments were performed in accordance with protocol approved by the Duke University Animal Care and Use Committee.

Bacterial strain and cell line

Clinical Uropathogenic *E. coli* isolate strain J96 was used for infection in mouse UTI model (6,75). The bacteria were statically grown overnight in Luria-Bertani broth 24 hours prior to infecting mouse. Primary human bladder epithelial cells (HBEP05) were purchased from CellnTec, and was grown in defined Keratinocyte SFM (ThermoFisher) and incubated at 37°C with 5% CO_2.

Mouse UTI model

UTI models from previous research were used (6). To induce cystitis, mice were given pentobarbital sodium (Oak Pharmaceuticals) i.p. for anesthesia, then 1×10^8 Uropathogenic *E. coli* strain J96 in 30μl PBS were slowly introduced into mouse bladder over a 2 min period through a 2cm catheter inserted into mouse urethra. A second cystitis was induced three weeks after the first one. To induce pyelonephritis, mice were given pentobarbital sodium i.p. for anesthesia, then 1×10^8 Uropathogenic *E. coli* strain J96 in 80μl PBS were quickly introduced into mouse bladder through a 2cm catheter inserted into mouse urethra. A second pyelonephritis was induced three weeks after the first one.

Bacteria load assessment

The bladders were collected at different time point post infection as indicated in the figure legends, and homogenized in 0.1% Triton X-100 (Sigma) by using zirconia silica beads for three cycles of 1.5 min each in an automatic homogenizer. Lysate underwent series dilution in PBS and was put on Difco MacConkey agar plate. After overnight incubation in 37 °C, colony forming unit (CFU) was counted.

FTY720 treatment

FTY720 treatment was modified from previous research (43, 76). Briefly, FTY720 (Sigma) was dissolved in distilled water following manufacture instruction. 1 mg/kg bodyweight FTY720 was i.p. injected into mice one day before bladder infection. Then it was injected daily till mice were euthanized.

Cross section and immunofluorescence staining

Bladders or lymph nodes were collected at different time point post infection as indicated in the figure legends, put into OCT compound, and immediately frozen. Then, 10um tissue sections were made in CM1850 Leica Biosystems cryostat (Leica Biosystems Inc) and put onto positive charged slides. The samples were then fixed in acetone for 20min in 4°C. After fixation, the samples were blocked with 1% anti-mouse CD16/CD32 (BD biosciences) or 5% Normal Donkey Serum (Sigma) and 1% BSA in PBS for 1 hour in room temperature. Bladder samples were incubated with 0.1% anti-cytokeratin 5 antibody (Abcam), 1% Anti-GATA3 antibody (ab106625, Abcam), 1% Anti-T-bet antibody (ab91109, Abcam), or 1% isotype control antibody overnight in 4°C, the next day, were incubated with 0.1% secondary antibody conjugated with fluorescence phore (Jackson ImmunoResearch), 1% anti-CD4 antibody conjugated with APC (BD biosciences), 1% anti-CD301b antibody conjugated with PE (Biolegend), or Anti-Mouse OX40L conjugated with Alexa Fluor 647(BD biosciences) for one hour in room temperature, light was avoided. Lymph node samples were incubated with 1% anti-CD11c antibody conjugated with FITC (BD biosciences), 1% anti-CD301b antibody conjugated with PE (Biolegend) and 1% anti-CD4 antibody conjugated with APC (Biolegend) for one hour in room temperature, light was avoided. The slides were mounted with Fluoroshield with DAPI reagent (Sigma) and examined using a Leica SP5 confocal microscope. The collected pictures were analyzed and quantified by ImageJ.

Flow cytometry analysis

Bladders, kidneys and lymph nodes were collected at different time point post infection as indicated in the figure legends. Single-cell suspensions were prepared as stated below, and light was avoided in the whole process. Bladder was digested with 1 mg/ml Collagenase (C7657; Sigma), 200 ug/ml DNase I (DN25; Sigma) in RPMI 1640 for 1 hour at 37°C. Kidney was digested with 1 mg/ml Collagenase (C7657; Sigma), 200 ug/ml DNase I (DN25; Sigma) in RPMI 1640 for 15min at 37°C. Lymph node was smashed and filtered through 70um cell strainer in FACS buffer (3% heat inactivated fetal bovine serum and 5mM EDTA in PBS). Samples were blocked with 1% Anti-mouse CD16/CD32 (BD biosciences), 5% normal mouse serum and 5% normal rat serum in FACS buffer for 15min at 4°C. Then, surface staining was performed with 7-AAD (BD biosciences) and the following antibodies. APC conjugated to anti-mouse TCR γ/δ (GL3), APC-Cy7 conjugated to anti-mouse CD8a (53–6.7) were from BioLegend. PE conjugated to anti-mouse Gr1 (RB6–8C5), PECy7 conjugated to anti-mouse CD3e (145–2C11), Pacific Blue conjugated to anti-mouse CD4 (RM4–5), BV510 conjugated to Anti-Mouse NK-1.1 (PK136), BB515 conjugated to anti-mouse CD326 (G8.8), FITC conjugated to anti-mouse CD11c (HL3), APC conjugated to anti-mouse CD11c (HL3), APC-Cy7 conjugated to anti-mouse CD45 (30-F11), BV510

conjugated to anti-mouse I-A/I-E (M5/114.15.2) were from BD Biosciences. All the samples were pre-gated by size and granularity based on forward and side scatter to select single cells, and then gated on 7-AAD negative cells. Data were collected by FACSCanto (BD Biosciences) and analyzed with FlowJo software (TreeStar).

ELISA

Bladders were collected at different time point post infection as indicated in the figure legends. Then bladders were homogenized by using zirconia silica beads for three cycles of 1.5 min each in an automatic homogenizer, and enzyme-linked immunosorbent assay was performed by using T_H1/T_H2 ELISA Kit (88–7711-44, ThermoFisher), IL-12p70 ELISA Kit (BMS6004, ThermoFisher), EGF ELISA Kit (EMEGF, ThermoFisher), IGF-1 ELISA Kit (EMIGF1, ThermoFisher), or TGFα ELISA Kit (EHTGFA, ThermoFisher) following manufacture's instruction. Concentrations were determined by standard curve. The level of IFN-γ and IL-4 at various time points was normalized to the level at day 0 without infection.

Dextran penetration and whole mount staining

Dextran penetration and whole mount staining were modified from previous research (22, 77). 1×10^8 CFU UPEC strain J96 were given to the mouse bladders to induce cystitis. On day 0, day 1 and day 3 post infection, 50ul dextran-Texas Red (1mg/ml in PBS, D1828, Invitrogen) was given into bladder through catheter inserted in urethra while mouse is under anesthesia. 30min after dextran delivery, mice were euthanized by CO_2 and bladders were collected. Bladders were cut from the middle to be fully unfolded and the whole epithelium was exposed. The samples were then fixed in 4% paraformaldehyde solution for 2 hours. Next, the samples were washed three times in PBS and incubated in blocking buffer (0.3% Triton, 5% donkey serum in 1% BSA-PBS solution) for 2 hours with shaking in room temperature. Then, samples will be incubated with anti-cytokeratin 5 antibody (1:200 dilution in blocking buffer, Abcam) overnight in 4°C. The next day, after washed three times with PBS, samples were further incubated with wheat germ agglutinin conjugated with FITC (1:200 dilution, Molecular Probes) and secondary donkey anti-rabbit antibody conjugated with Alexa Fluor 647 (1:1000 dilution, Jackson ImmunoReseaerch) in blocking buffer for 2 hours in room temperature. Then they were washed in PBS twice, mounted on slides with ProLong Gold antifade mounting agent. Slides were examined using a Leica SP5 confocal microscope. The collected pictures were analyzed and quantified by ImageJ.

Trypan blue assay

1×10^8 CFU UPEC strain J96 were given to the mouse bladders to induce cystitis. Trypan blue assay was then performed based on previous research (78). Briefly, on Day 0, Day 1 and Day 3 post infection, 1% trypan blue in PBS (50ul) was slowly given into bladder through a catheter inserted in mouse urethra while mouse is under anesthesia. 30min after trypan blue delivery, bladder were collected and pictures were taken on the bladders. The trypan blue intensity was measured in ImageJ, and the intensity on Day 1 and Day 3 was normalized to the intensity on Day 0.

CD4 T cell *in vitro* differentiation and adoptive transfer

For T_H0 and T_H2 cell culture experiment, 1×10^8 E.coli J96 in 30μl PBS were delivered into the bladders of 4get mice to induce cystitis. A second infection was given two weeks after the first one in the same way. Three days after the second infection, the iliac lymph nodes were collected, smashed and filtered through 70μm cell strainer. Then CD4 T cells were concentrated by EasySep Mouse CD4+ T Cell Isolation Kit (19852, Stemcell). The concentrated CD4 T cells were immediately seeded in anti-CD3/anti-CD28 antibodies (BD bisosciences) coated plate in RPMI 1640 with 10% heat inactivated fetal bovine serum. 10μg/mL anti-IFN-γ antibody (BD bisosciences), 1μg/mL IL-2 (Biolegend) and 1μg/mL IL-4 (Biolegend) were added to polarize the CD4 T cells for Th2 culture; 1μg/mL IL-2 (Biolegend) was added for T_H0 culture. Cells were cultured for four days at 37°C with 5% CO_2. The cells were harvest on day 4, and T_H2 polarity was assessed by flow cytometry. Then 1×10^6 cells in 100μl PBS were i.v. injected into each *Il4*$^{-/-}$ mouse. For sorting-out T_H2 cell experiment, 1×10^7 *E.coli* J96 in 100ul PBS were i.p. delivered into 4get mice. A second infection was given two weeks after the first one in the same way. Two days after the second infection, lymph nodes and spleen were collected, smashed and filtered through 70μm cell strainer. Then CD4 T cells were concentrated by EasySep Mouse CD4+ T Cell Isolation Kit (19852, Stemcell) and GFP+ cells were sorted out by Sony SH800 cell sorter. 1×10^5 GFP$^+$ cells were i.v. injected into each *Il4*$^{-/-}$ mouse. As control, CD4 T cells isolated from iliac lymph nodes of naïve 4get mice were stimulated by anti-CD3/anti-CD28 antibodies and cultured under T_H2 condition for four days. 1×10^5 GFP$^+$ cells were sorted out from the cultured cells and i.v. injected into *Il4*$^{-/-}$ mouse. For sorting-out Th1 cell experiment, 1×10^7 *E.coli* J96 in 100ul PBS were i.p. delivered into Great mice. A second infection was given two weeks after the first one in the same way. Two days after the second infection, lymph nodes and spleen were collected, smashed and filtered through 70μm cell strainer. Then CD4 T cells were concentrated by EasySep Mouse CD4+ T Cell Isolation Kit (19852, Stemcell) and YFP+ cells were sorted out by Sony SH800 cell sorter. $2X10^5$ YFP+ cells were i.v. injected into each *Ifng*$^{-/-}$ mouse.

RT-PCR

Bladders were collected at different time point post infection as indicated in the figure legends. Total RNA was extracted by using RNeasy mini kit (Qiagen) following manufacture's instruction. 1ug extracted RNA was used to synthesize cDNA in a 20ul solution system by using SuperScript IV Reverse Transcriptase (ThermoFisher) and Oligo $d(T)_{20}$ (ThermoFisher). Synthesized cDNA was 1:10 diluted in DNAase and RNAase free water. 5ul cDNA dilution was then used for RT-PCR with iQ SYBR Green Supermix (1708882, Bio-Rad), following manufacture's instruction. The PCR reactions were initiated with denaturation at 95°C for 3 min; followed by 40 amplification cycles at 95°C for 15 s and 60°C for 30 s. Samples were run in duplicate, data were collected in LightCycler 480 Instrument II (Roche) and analyzed by software LightCycler 480 sw 1.5.1 (Roche).

Gene expression level was normalized to either uninfected samples or Wt samples as indicated in the figure legends. The following primers were used based on previous publications. EGF-F: 5'-AGAGCCAGTTCAGTAGAAACTGGG-3', EGF-R: 5'-ACTTTGGTTTCTAATGATTTTCTCC-3' (79); HB-EGF-F: 5'-

ATGAAGCTGCTGCCGTCGGTGATGCTGA-3', HB-EGF-R: 5'-GGTATCTGCACTCCCCGTGGATGC-3' (80); TGFα-F: 5'-CCAGATTCCCACACTCAGT-3', TGFα-R: 5'-GGAGGTCTGCATGCTCACA-3' (81); IGF1-F: 5'-GTCTTCACACCTCTTCTACC-3', IGF1-R: 5'-CCTTCTGAGTCTTGGGCATGTCAG-3' (82); IGF2-F: 5'-TCCTGTCTTCATCCTCTTCCAGCCCC-3', IGF2-R: 5'-CGGTCCGAACAGACAAACTGAAGCGT-3' (83); Arg1-F: 5'-CTCCAAGCCAAAGTCCTTAGAG-3', Arg1-R: 5'-AGGAGCTGTCATTAGGGACATC-3' (84); Fizz1-F: 5'-TCCCAGTGAATACTGATGAGA-3', Fizz1-R: 5'-CCACTCTGGATCTCCCAAGA-3' (52); Ym1-F: 5'-AGAAGGGAGTTTCAAACCTGGT-3', Ym1-R: 5'-GTCTTGCTCATGTGTGTAAGTGA-3' (84); b-actin-F: 5'-GATTACTGCTCTGGCTCCTAGC-3', b-actin-R: 5'-GACTCATCGTACTCCTGCTTGC-3' (6).

BrdU assay

Primary human bladder epithelial cells were seeded on 22×22 mm glass coverslips and were cultured with 10uM 5-Bromo-2'-deoxyuridine (Sigma) and different concentrations of various growth factors as indicated in the figure legends for 24 hours in Keratinocyte SFM medium. The next day, the cells were fixed in 4% paraformaldehyde and permeabilized in blocking buffer (0.1% saponin, 1% fish gelatin, 5% normal mouse serum in PBS) for 30 min in room temperature. Then the samples were incubated in 1M HCL for 1 hour at room temperature, followed by three times PBS wash and another 30 min incubation with blocking buffer. The cells were then incubated with FITC conjugated Mouse Anti-Human BrdU antibody with DNase (1:100 dilution in blocking buffer) overnight in 4°C. Then coverslips were mounted with Fluoroshield with DAPI reagent (Sigma) and examined using a Leica SP5 confocal microscope. In ImageJ, the cells with positive staining of BrdU were counted.

GW2580 treatment

GW2580 treatment was performed as described by previous research(54–56). GW2580 (Sigma) suspended in 0.5% hydroxypropylmethylcellulose and 0.1% Tween 80 or vehicle solution alone was delivered at 50mg/kg bodyweight twice everyday by oral gavage. The delivery was started one day before infection and continued till mice were euthanized.

CD301b$^+$ DC knock-out

CD301b$^+$ DC knock-out was performed following the previous publication (57, 58). Briefly, 500ng DT in 100ul PBS were i.p. given to CD301b-DTR mice. Two days later, 1×10^8 J96 in 30ul PBS were delivered into the mouse bladders to induce cystitis. The day with J96 delivery was referred as Day 0. Bladders and lymph nodes were collected at Day 0, Day 1, Day 3 for flow cytometry analysis. CD301b$^+$ DC depletion was confirmed by flow cytometry on Day 0 and Day 3 as shown in supplementary information. For a second infection, DT treatment was continued once a week between the first and second infection.

Ligand neutralization

200μg anti-ICOSL, anti-PD-L2, anti-OX40L or a collection of isotype control antibodies were i.p. injected into 4get or Great mice. 24h later, UPEC strain J96 (1×10^8 CFU) was administered to the bladders of these mice and antibodies were i.p. injected again. Another three days later, bladders were collected for flow cytometry analysis.

Cystometry

$CD301b^+$ DC knock-out was performed following the previous research (85, 86). 8–10 week old female C57BL/6J mice were infected once weekly for three total infections. 14 days or 2 months following the third infection, cystometry was performed in conscious restrained mice. Briefly, PE-10 catheters were implanted into the bladder dome of mice 7 days before cystometry. The catheter was routed from the bladder to the interscapular region and sealed. For cystometry, mice were restrained using a Ballman-type restrainer (Natsume Seisakusho Co., Tokyo, Japan) and placed inside a Small Animal Cystometry Lab Station (Med Associates, St. Albans, VT). An analytical balance was used to measure void volume. Saline was infused into the bladder at a fixed rate of 15 uL/min for 2 hours by utilizing a syringe pump equipped with an in-line pressure transducer. Scale and pressure measurements were recorded with Med-CMG software (Med Associates). At least 10 voiding cycles were recorded. CMG Analysis software (version 1.06; Med Associates) was used to analyze void frequency, defined as the number of voids per hour, and void volume, defined as the amount of change on the analytical balance.

Repeated infections and epithelium thickness measurement

1×10^8 CFU UPEC strain J96 were intravesically administered to induce cystitis once every week for three times. PBS was intravesically administered in control mice. At various time points after the final infections, cystometry, flow cytometry, or cross section were performed. For measurement of epithelium thickness, cross section and immunofluorescence staining were done on bladder samples. Then, Measurement was performed by ImageJ on pictures obtained from Leica SP5 confocal microscope. The thickness from the top of superficial BEC layer to where BEC staining ends was measured. DAPI staining is also used as a reference for the thickness measurement.

Statistics and reproducibility

Statistical analyses were performed using v.8.4.1 (GraphPad Software, La Jolla, CA, USA). A two-tailed unpaired t test was used for comparison between two groups; An ordinary ANOVA with a post test corrected for multiple comparison was used for comparisons among more than two groups. Each experiment was repeated independently with similar results for two to three times. Detailed information is in each figure legend. $p<0.05$ was considered statistically significant. Post-test p values are as follows: * $p < 0.05$; ** $p < 0.01$; *** $p < 0.001$, **** $p < 0.0001$

Data availability statement

All data supporting the findings of this study are available within the article and its supplementary information and from the corresponding author upon reasonable request.

Supplementary Material

Refer to Web version on PubMed Central for supplementary material.

ACKNOWLEDGMENTS

We thank Dr. Richard Locksley for providing the reporter strains. We thank Duke Light Microscopy Core Facility (LMCF), especially Dr. Yasheng Gao, for their expertise and advice in light microscopy imaging. We thank The Flow Cytometry Shared Resource (FCSR) of Duke Cancer Institute for their assistance with flow cytometry analysis. We also appreciate Dr. Min-Nung Huang's help in the design of flow cytometry panel. The authors' work is supported by the US National Institutes of Health grants R21CA223093, R01DK121032, R01DK101456 and R56AI139620 to SNA.

References

1. Foxman B, Barlow R, D'Arcy H, et al. Urinary tract infection: selfreported incidence and associated costs. Ann Epidemiol. 2000;10:509–15. [PubMed: 11118930]
2. Silverman JA, Schreiber HL, Hooton TM, Hultgren SJ. From physiology to pharmacy: developments in the pathogenesis and treatment of recurrent urinary tract infections. Current urology reports. 2013 10 1;14(5):448–56. [PubMed: 23832844]
3. Foxman B. Urinary tract infection syndromes: occurrence, recurrence, bacteriology, risk factors, and disease burden. Infectious disease clinics of North America. 2014 3 31;28(1):1–3. [PubMed: 24484571]
4. Al-Badr A, Al-Shaikh G. Recurrent urinary tract infections management in women: a review. Sultan Qaboos University Medical Journal. 2013 8;13(3):359. [PubMed: 23984019]
5. Flores-Mireles AL, Walker JN, Caparon M, Hultgren SJ. Urinary tract infections: epidemiology, mechanisms of infection and treatment options. Nature reviews microbiology. 2015 5;13(5):269. [PubMed: 25853778]
6. Chan CY, John AL, Abraham SN. Mast cell interleukin-10 drives localized tolerance in chronic bladder infection. Immunity. 2013 2 21;38(2):349–59. [PubMed: 23415912]
7. Hooton TM. Recurrent urinary tract infection in women. International journal of antimicrobial agents. 2001 4 1;17(4):259–68. [PubMed: 11295405]
8. Foxman B. Recurring urinary tract infection: incidence and risk factors. American journal of public health. 1990 3;80(3):331–3. [PubMed: 2305919]
9. Ikähelmo R, Siitonen A, Heiskanen T, Kärkkäinen U, Kuosmanen P, Lipponen P, Mäkelä PH. Recurrence of Urinary Tract Infection in a Primary Care Setting: Analysis of a I-Year Follow-up of 179 Women. Clinical Infectious Diseases. 1996 1 1;22(1):91–9. [PubMed: 8824972]
10. Kaye MG, Fox MJ, Bartlett JG, Braman SS, Glassroth J. The clinical spectrum of Staphylococcus aureus pulmonary infection. Chest. 1990 4 1;97(4):788–92. [PubMed: 2323247]
11. Mogulkoc N, Karakurt S, Isalska B, Bayindir U, Çelikel T, Korten V, Çolpan N. Acute purulent exacerbation of chronic obstructive pulmonary disease and Chlamydia pneumoniae infection. American journal of respiratory and critical care medicine. 1999 7 1;160(1):349–53. [PubMed: 10390424]
12. Caminero JA, Pena MJ, Campos-Herrero MI, RodrÍguez JC, Afonso O, Martin C, PavÓn JM, Torres MJ, Burgos M, Cabrera P, Small PM. Exogenous reinfection with tuberculosis on a European island with a moderate incidence of disease. American journal of respiratory and critical care medicine. 2001 3 1;163(3):717–20. [PubMed: 11254530]
13. Zar FA, Bakkanagari SR, Moorthi KM, Davis MB. A comparison of vancomycin and metronidazole for the treatment of Clostridium difficile–associated diarrhea, stratified by disease severity. Clinical Infectious Diseases. 2007 8 1;45(3):302–7. [PubMed: 17599306]
14. Borody TJ, Cole P, Noonan S, Morgan A, Lenne J, Hyland L, Brandl S, Borody EG, George LL. Recurrence of duodenal ulcer and Campylobacter pylori infection after eradication. Medical Journal of Australia. 1989 10;151(8):431–5. [PubMed: 2687668]

15. Niv Y, Hazazi R. Helicobacter pylori recurrence in developed and developing countries: meta-analysis of 13C-urea breath test follow-up after eradication. Helicobacter. 2008 2;13(1):56–61. [PubMed: 18205667]
16. Abraham SN, Miao Y. The nature of immune responses to urinary tract infections. Nature Reviews Immunology. 2015 10 1;15(10):655–63.
17. Wu J, Miao Y, Abraham SN. The multiple antibacterial activities of the bladder epithelium. Annals of translational medicine. 2017 1;5(2).
18. Haraoka M, Hang L, Frendéus B, Godaly G, Burdick M, Strieter R, Svanborg C. Neutrophil recruitment and resistance to urinary tract infection. The Journal of infectious diseases. 1999 10 1;180(4):1220–9. [PubMed: 10479151]
19. Schiwon M, Weisheit C, Franken L, Gutweiler S, Dixit A, Meyer-Schwesinger C, Pohl JM, Maurice NJ, Thiebes S, Lorenz K, Quast T. Crosstalk between sentinel and helper macrophages permits neutrophil migration into infected uroepithelium. Cell. 2014 1 30;156(3):456–68. [PubMed: 24485454]
20. Tittel AP, Heuser C, Ohliger C, Knolle PA, Engel DR, Kurts C. Kidney dendritic cells induce innate immunity against bacterial pyelonephritis. Journal of the American Society of Nephrology. 2011 8 1;22(8):1435–41. [PubMed: 21757770]
21. Mulvey MA, Schilling JD, Hultgren SJ. Establishment of a persistent Escherichia coli reservoir during the acute phase of a bladder infection. Infection and immunity. 2001 7 1;69(7):4572–9. [PubMed: 11402001]
22. Choi HW, Bowen SE, Miao Y, Chan CY, Miao EA, Abrink M, Moeser AJ, Abraham SN. Loss of bladder epithelium induced by cytolytic mast cell granules. Immunity. 2016 12 20;45(6):1258–69. [PubMed: 27939674]
23. Percival A, Brumfitt W, De Louvois J. Serum-antibody levels as an indication of clinically inapparent pyelonephritis. The Lancet. 1964 11 14;284(7368):1027–33.
24. Sanford BA, Thomas VL, Forland MA, Carson SA, Shelokov AL. Immune response in urinary tract infection determined by radioimmunoassay and immunofluorescence: serum antibody levels against infecting bacterium and Enterobacteriaceae common antigen. Journal of clinical microbiology. 1978 11 1;8(5):575–9. [PubMed: 83326]
25. Clark H, Ronald AR, Turck M. Semm Antibody Response in Renal Versus Bladder Bacteriuria. Journal of Infectious Diseases. 1971 5 1;123(5):539–43. [PubMed: 5000471]
26. McCue JD. The management of complicated urinary tract infections. Infect. Dis. 2004;22:55–65.
27. Ramakrishnan K, Scheid DC. Diagnosis and management of acute pyelonephritis in adults. Am Fam Physician. 2005 3 1;71(5):933–42. [PubMed: 15768623]
28. Jones-carson J, Balish E, Uehling DT. Susceptibility of immunodeficient gene-knockout mice to urinary tract infection. The Journal of urology. 1999 1;161(1):338–41. [PubMed: 10037434]
29. Thumbikat P, Waltenbaugh C, Schaeffer AJ, Klumpp DJ. Antigen-specific responses accelerate bacterial clearance in the bladder. The Journal of Immunology. 2006 3 1;176(5):3080–6. [PubMed: 16493067]
30. Mora-Bau G, Platt AM, van Rooijen N, Randolph GJ, Albert ML, Ingersoll MA. Macrophages subvert adaptive immunity to urinary tract infection. PLoS pathogens. 2015 7 16;11(7):e1005044.
31. Sivick KE, Schaller MA, Smith SN, Mobley HL. The innate immune response to uropathogenic Escherichia coli involves IL-17A in a murine model of urinary tract infection. The journal of immunology. 2010 2 15;184(4):2065–75. [PubMed: 20083670]
32. Curtsinger JM, Mescher MF. Inflammatory cytokines as a third signal for T cell activation. Current opinion in immunology. 2010 6 1;22(3):333–40. [PubMed: 20363604]
33. Flynn S, Toellner KM, Raykundalia C, Goodall M, Lane P. CD4 T cell cytokine differentiation: the B cell activation molecule, OX40 ligand, instructs CD4 T cells to express interleukin 4 and upregulates expression of the chemokine receptor, Blr-1. Journal of Experimental Medicine. 1998 7 20;188(2):297–304. [PubMed: 9670042]
34. Macatonia SE, Hosken NA, Litton M, Vieira P, Hsieh CS, Culpepper JA, Wysocka M, Trinchieri G, Murphy KM, O'Garra A. Dendritic cells produce IL-12 and direct the development of Th1 cells from naive CD4+ T cells. The Journal of Immunology. 1995 5 15;154(10):5071–9. [PubMed: 7730613]

35. Croft M, Bradley LM, Swain SL. Naive versus memory CD4 T cell response to antigen. Memory cells are less dependent on accessory cell costimulation and can respond to many antigen-presenting cell types including resting B cells. The Journal of Immunology. 1994 3 15;152(6):2675–85. [PubMed: 7908301]
36. Croft M, Swain SL. Recently activated naive CD4 T cells can help resting B cells, and can produce sufficient autocrine IL-4 to drive differentiation to secretion of T helper 2-type cytokines. The Journal of Immunology. 1995 5 1;154(9):4269–82. [PubMed: 7536767]
37. Julia V, McSorley SS, Malherbe L, Breittmayer JP, Girard-Pipau F, Beck A, Glaichenhaus N. Priming by microbial antigens from the intestinal flora determines the ability of CD4+ T cells to rapidly secrete IL-4 in BALB/c mice infected with Leishmania major. The Journal of Immunology. 2000 11 15;165(10):5637–45. [PubMed: 11067920]
38. Hegazy AN, West NR, Stubbington MJ, Wendt E, Suijker KI, Datsi A, This S, Danne C, Campion S, Duncan SH, Owens BM. Circulating and tissue-resident CD4+ T cells with reactivity to intestinal microbiota are abundant in healthy individuals and function is altered during inflammation. Gastroenterology. 2017 11 1;153(5):1320–37. [PubMed: 28782508]
39. Farber DL, Yudanin NA, Restifo NP. Human memory T cells: generation, compartmentalization and homeostasis. Nature Reviews Immunology. 2014 1;14(1):24–35.
40. Honda K, Littman DR. The microbiota in adaptive immune homeostasis and disease. Nature. 2016 7;535(7610):75–84. [PubMed: 27383982]
41. Williams WB, Han Q, Haynes BF. Cross-reactivity of HIV vaccine responses and the microbiome. Current Opinion in HIV and AIDS. 2018 1;13(1):9–14. [PubMed: 29035947]
42. Su LF, Kidd BA, Han A, Kotzin JJ, Davis MM. Virus-specific CD4+ memory-phenotype T cells are abundant in unexposed adults. Immunity. 2013 2 21;38(2):373–83. [PubMed: 23395677]
43. Sawicka E, Zuany-Amorim C, Manlius C, Trifilieff A, Brinkmann V, Kemeny DM, Walker C. Inhibition of Th1-and Th2-mediated airway inflammation by the sphingosine 1-phosphate receptor agonist FTY720. The Journal of Immunology. 2003 12 1;171(11):6206–14. [PubMed: 14634137]
44. Reinhardt RL, Liang HE, Locksley RM. Cytokine-secreting follicular T cells shape the antibody repertoire. Nature immunology. 2009 4 1;10(4):385–93. [PubMed: 19252490]
45. Reinhardt RL, Liang HE, Bao K, Price AE, Mohrs M, Kelly BL, Locksley RM. A novel model for IFN-γ–mediated autoinflammatory syndromes. The Journal of Immunology. 2015 3 1;194(5):2358–68. [PubMed: 25637019]
46. Mohrs M, Shinkai K, Mohrs K, Locksley RM. Analysis of type 2 immunity in vivo with a bicistronic IL-4 reporter. Immunity. 2001 8 1;15(2):303–11. [PubMed: 11520464]
47. Hopkins WJ, Gendron-Fitzpatrick A, Balish E, Uehling DT. Time course and host responses to Escherichia coli urinary tract infection in genetically distinct mouse strains. Infection and immunity. 1998 6 1;66(6):2798–802. [PubMed: 9596750]
48. Wynn TA. Type 2 cytokines: mechanisms and therapeutic strategies. Nature Reviews Immunology. 2015 5;15(5):271.
49. Walker JA, McKenzie AN. TH2 cell development and function. Nature Reviews Immunology. 2018 2;18(2):121.
50. Murray PJ, Wynn TA. Protective and pathogenic functions of macrophage subsets. Nature reviews immunology. 2011 11;11(11):723.
51. Chen F, Liu Z, Wu W, Rozo C, Bowdridge S, Millman A, Van Rooijen N, Urban JF Jr, Wynn TA, Gause WC. An essential role for TH2-type responses in limiting acute tissue damage during experimental helminth infection. Nature medicine. 2012 2 1;18(2):260–6.
52. Raes G, De Baetselier P, Noël W, Beschin A, Brombacher F, Gh GH. Differential expression of FIZZ1 and Ym1 in alternatively versus classically activated macrophages. Journal of leukocyte biology. 2002 4 1;71(4):597–602. [PubMed: 11927645]
53. Gordon S, Martinez FO. Alternative activation of macrophages: mechanism and functions. Immunity. 2010 5 28;32(5):593–604. [PubMed: 20510870]
54. Conway JG, McDonald B, Parham J, Keith B, Rusnak DW, Shaw E, Jansen M, Lin P, Payne A, Crosby RM, Johnson JH. Inhibition of colony-stimulating-factor-1 signaling in vivo with the orally bioavailable cFMS kinase inhibitor GW2580. Proceedings of the National Academy of Sciences. 2005 11 1;102(44):16078–83.

55. He H, Xu J, Warren CM, Duan D, Li X, Wu L, Iruela-Arispe ML. Endothelial cells provide an instructive niche for the differentiation and functional polarization of M2-like macrophages. Blood. 2012 10;120(15):3152–62 [PubMed: 22919031]
56. Klinkert K, Whelan D, Clover AJ, Leblond AL, Kumar AH, Caplice NM. Selective M2 macrophage depletion leads to prolonged inflammation in surgical wounds. European Surgical Research. 2017;58(3–4):109–20. [PubMed: 28056458]
57. Kumamoto Y, Linehan M, Weinstein JS, Laidlaw BJ, Craft JE, Iwasaki A. CD301b+ dermal dendritic cells drive T helper 2 cell-mediated immunity. Immunity. 2013 10 17;39(4):733–43. [PubMed: 24076051]
58. Kumamoto Y, Denda-Nagai K, Aida S, Higashi N, Irimura T. MGL2+ dermal dendritic cells are sufficient to initiate contact hypersensitivity in vivo. PloS one. 2009 5 19;4(5):e5619.
59. Gao Y, Nish SA, Jiang R, Hou L, Licona-Limón P, Weinstein JS, Zhao H, Medzhitov R. Control of T helper 2 responses by transcription factor IRF4-dependent dendritic cells. Immunity. 2013 10 17;39(4):722–32. [PubMed: 24076050]
60. Connor LM, Tang SC, Camberis M, Le Gros G, Ronchese F. Helminth-conditioned dendritic cells prime CD4+ T cells to IL-4 production in vivo. The Journal of Immunology. 2014 9 15;193(6):2709–17. [PubMed: 25108019]
61. Sokol CL, Camire RB, Jones MC, Luster AD. The chemokine receptor CCR8 promotes the migration of dendritic cells into the lymph node parenchyma to initiate the allergic immune response. Immunity. 2018 9 18;49(3):449–63. [PubMed: 30170811]
62. Amsen D, Blander JM, Lee GR, Tanigaki K, Honjo T, Flavell RA. Instruction of distinct CD4 T helper cell fates by different notch ligands on antigen-presenting cells. Cell. 2004 5 14;117(4):515–26. [PubMed: 15137944]
63. Zhu J, Yamane H, Paul WE. Differentiation of effector CD4 T cell populations. Annual review of immunology. 2009 4 23;28:445–89.
64. Zhu J, Paul WE. CD4 T cells: fates, functions, and faults. Blood. 2008 9 1;112(5):1557–69. [PubMed: 18725574]
65. Fields PE, Kim ST, Flavell RA. Cutting edge: changes in histone acetylation at the IL-4 and IFN-γ loci accompany Th1/Th2 differentiation. The Journal of Immunology. 2002 7 15;169(2):647–50. [PubMed: 12097365]
66. Bashyam H. Th1/Th2 cross-regulation and the discovery of IL-10. Journal of Experimental Medicine. 2007 2 19;204(2):237-. [PubMed: 17354288]
67. Brubaker L, Wolfe A. The urinary microbiota: a paradigm shift for bladder disorders?. Current opinion in obstetrics & gynecology. 2016 10;28(5):407. [PubMed: 27379439]
68. Antunes-Lopes T, Vale L, Coelho AM, Silva C, Rieken M, Geavlete B, Rashid T, Rahnama'i SM, Cornu JN, Marcelissen T. The role of urinary microbiota in lower urinary tract dysfunction: a systematic review. European urology focus. 2018 9 28.
69. Yeung CK, Sreedhar B, Leung YF, Sit KY. Correlation between ultrasonographic bladder measurements and urodynamic findings in children with recurrent urinary tract infection. BJU international. 2007 3;99(3):651–5. [PubMed: 17092286]
70. Shaikh N, Hoberman A, Keren R, Gotman N, Docimo SG, Mathews R, Bhatnagar S, Ivanova A, Mattoo TK, Moxey-Mims M, Carpenter MA. Recurrent urinary tract infections in children with bladder and bowel dysfunction. Pediatrics. 2016 1;137(1).
71. Cho M, Lee J-E, Lim H, Shin H-W, Khalmuratova R, Choi G, et al. Fibrinogen cleavage products and Toll-like receptor 4 promote the generation of programmed cell death 1 ligand 2–positive dendritic cells in allergic asthma. Journal of Allergy and Clinical Immunology. 2018;142(2):530–41. [PubMed: 29038008]
72. Arifuzzaman M, Mobley YR, Choi HW, Bist P, Salinas CA, Brown ZD, et al. MRGPR-mediated activation of local mast cells clears cutaneous bacterial infection and protects against reinfection. Science advances. 2019 1 1;5(1):eaav0216.
73. O'Brien VP, Hannan TJ, Yu L, Livny J, Roberson ED, Schwartz DJ, Souza S, Mendelsohn CL, Colonna M, Lewis AL, Hultgren SJ. A mucosal imprint left by prior Escherichia coli bladder infection sensitizes to recurrent disease. Nature microbiology. 2017 1;2(1):16196.

74. O'Brien VP, Dorsey DA, Hannan TJ, Hultgren SJ. Host restriction of Escherichia coli recurrent urinary tract infection occurs in a bacterial strain-specific manner. PLoS pathogens. 2018 12 13;14(12):e1007457.

Methods-only References

75. Normark S, Lark D, Hull R, Norgren M, Båga M, O'Hanley P, Schoolnik G, Falkow S. Genetics of digalactoside-binding adhesin from a uropathogenic Escherichia coli strain. Infection and immunity. 1983 9 1;41(3):942–9. [PubMed: 6136465]

76. Di Pilato M, Kim EY, Cadilha BL, Prüßmann JN, Nasrallah MN, Seruggia D, Usmani SM, Misale S, Zappulli V, Carrizosa E, Mani V. Targeting the CBM complex causes T reg cells to prime tumours for immune checkpoint therapy. Nature. 2019 6;570(7759):112. [PubMed: 31092922]

77. Geesala R, Schanz W, Biggs M, Dixit G, Skurski J, Gurung P, Meyerholz DK, Elliott D, Issuree PD, Maretzky T. Loss of RHBDF2 results in an early-onset spontaneous murine colitis. Journal of leukocyte biology. 2019 4;105(4):767–81. [PubMed: 30694569]

78. Levin RM, Wein AJ, Whitmore K, Monson FC, Mc Kenna BA, Ruggieri MR. Trypan blue as an indicator of urothelial integrity. Neurourology and Urodynamics. 1990;9(3):269–79.

79. Warburton D, Seth R, Shum L, Horcher PG, Hall FL, Werb Z, Slavkin HC. Epigenetic role of epidermal growth factor expression and signalling in embryonic mouse lung morphogenesis. Developmental biology. 1992 1 1;149(1):123–33. [PubMed: 1728582]

80. Troyer KL, Luetteke NC, Saxon ML, Qiu TH, Xian CJ, Lee DC. Growth retardation, duodenal lesions, and aberrant ileum architecture in triple null mice lacking EGF, amphiregulin, and TGF-α. Gastroenterology. 2001 7 1;121(1):68–78. [PubMed: 11438495]

81. Marjou AE, Delouvée A, Thiery JP, Radvanyi F. Involvement of epidermal growth factor receptor in chemically induced mouse bladder tumour progression. Carcinogenesis. 2000 12 1;21(12):2211–8. [PubMed: 11133810]

82. Powell-Braxton L, Hollingshead P, Warburton C, Dowd M, Pitts-Meek S, Dalton D, Gillett N, Stewart TA. IGF-I is required for normal embryonic growth in mice. Genes & development. 1993 12 1;7(12b):2609–17. [PubMed: 8276243]

83. Leighton PA, Ingram RS, Eggenschwiler J, Efstratiadis A, Tilghman SM. Disruption of imprinting caused by deletion of the H19 gene region in mice. Nature. 1995 5;375(6526):34. [PubMed: 7536897]

84. Lumeng CN, Bodzin JL, Saltiel AR. Obesity induces a phenotypic switch in adipose tissue macrophage polarization. The Journal of clinical investigation. 2007 1 2;117(1):175–84. [PubMed: 17200717]

85. Inouye BM, Hughes FM Jr, Jin H, Lütolf R, Potnis KC, Routh JC, Rouse DC, Foo WC, Purves JT. Diabetic bladder dysfunction is associated with bladder inflammation triggered through hyperglycemia, not polyuria. Research and reports in urology. 2018;10:219. [PubMed: 30533402]

86. Hughes FM, Hirshman NA, Inouye BM, Jin H, Stanton EW, Yun CE, Davis LG, Routh JC, Purves JT. NLRP3 promotes diabetic bladder dysfunction and changes in symptom-specific bladder innervation. Diabetes. 2019 2 1;68(2):430–40. [PubMed: 30425063]

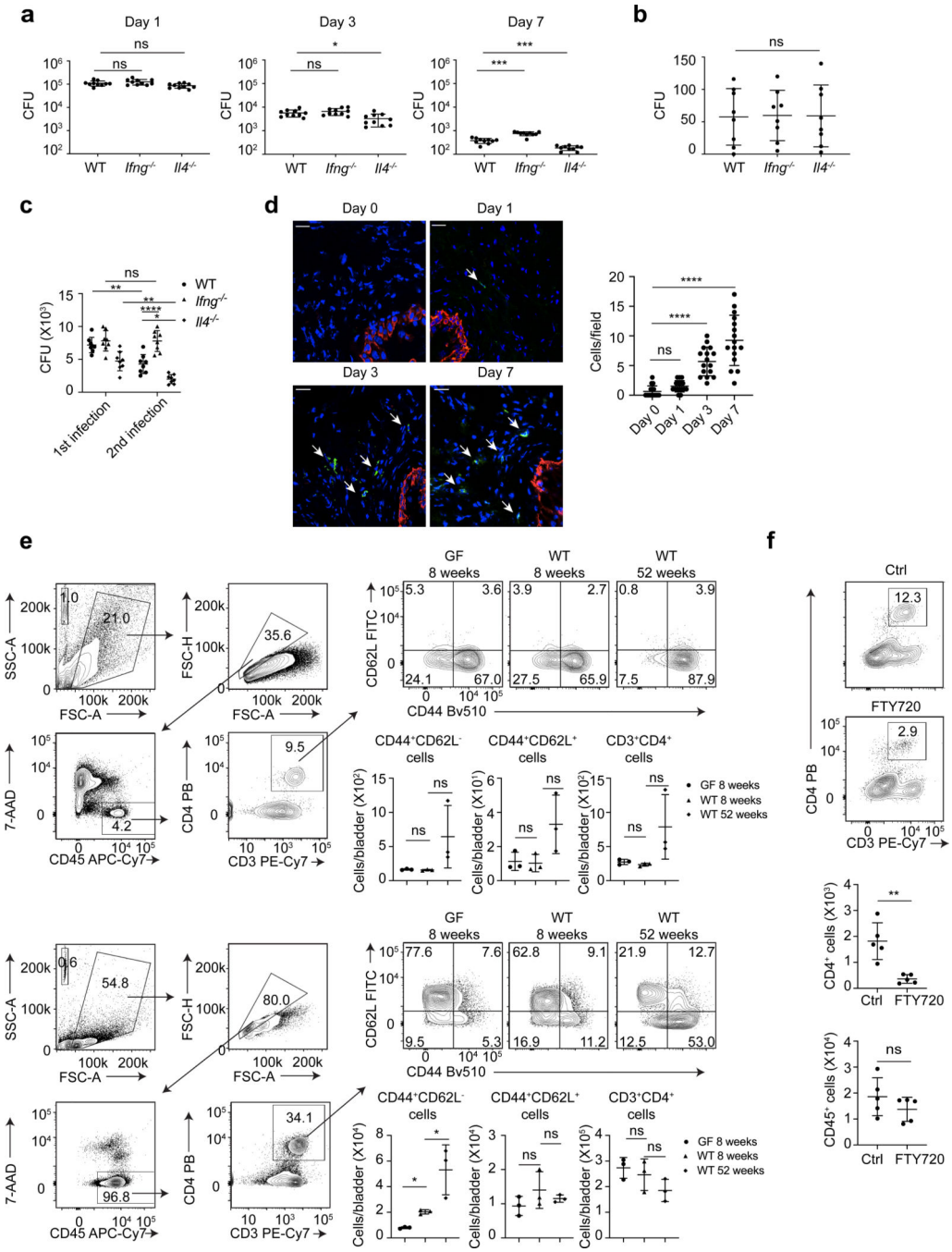

Figure 1. *Il4*$^{-/-}$ but not *Ifng*$^{-/-}$ mice initiate bacteria clearance within three days post bladder infection.

a, UPEC was administered into the bladders of WT, *Ifng*$^{-/-}$ or *Il4*$^{-/-}$ mice. Bacterial load of the whole bladder was assessed on Day 1, 3, and 7 post infection, n=10 mice per group. **b**, Bacterial load was assessed three weeks after infection, n=7 mice. **c**, Three weeks after the first infection, a second infection was given to the mice. Bacterial load was assessed on Day 3 after the first and second infections, n=8 mice. **d**, Bladders were collected on Day 0, 1, 3 and 7 post infection for cross section and immunofluorescence staining of nuclei (DAPI,

blue), uroepithelium (cytokeratin 5, red) and CD4 T cells (CD4, green). White arrow indicates CD4 T cells. White bar marks 25μm. CD4 T cell numbers per field were counted (right). n=16 field, and each group has 4 mice. **e**, Three bladders (upper panels) or six BLNs (lower panels) from GF 8-week-old C57BL/6J mice, WT 8-week-old C57BL/6J mice, or WT 52-week-old C57BL/6J mice were pooled for flow cytometry analysis. Gating strategy is shown in the left, and quantified cell number are shown below the flow cytometry plot. Each data point represents the average number in a single pool and n= 9 mice. **f**, FTY720 or dH_2O alone was injected intraperitoneally, then mouse bladders were infected by UPEC (Day 0) and collected for flow cytometry analysis on Day 3. Gating strategy is the same as **e**. Quantification of cell numbers is shown below. Data represent three independent experiments and are shown as mean ± SD. Data were analyzed by an ordinary one-way ANOVA with a Dunnett's post-test comparing each group with a control group (**a**, **b**, **d**, **e**), an ordinary two-way ANOVA with a Turkey's multiple comparison post-test (**c**), or an unpaired two-tail t test (**f**). *p<0.05, **p<0.01, ***p<0.001, ****p<0.0001, ns=not significant.

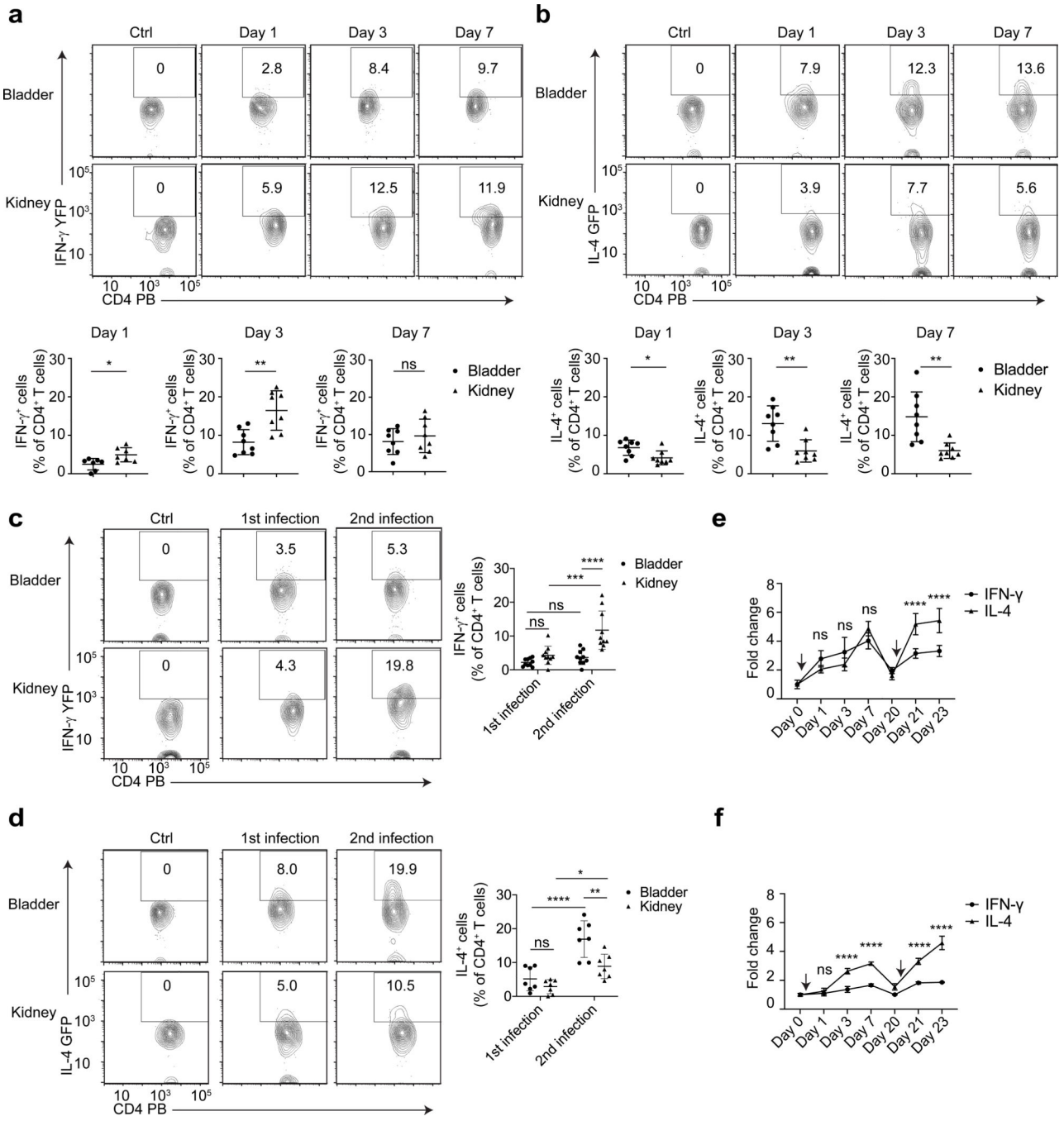

Figure 2. CD4 T cells are preferentially differentiated into T_H2 cells in the bladder particularly after a second infection.

UPEC was administered into the bladders and kidneys of Great mice (**a**) or 4get mice (**b**), and on Day 1, 3, 7 post infection, bladders and kidneys were collected for flow cytometry analysis. WT C57BL/6J mice intravesically infected with UPEC for three days serve as negative control for fluorescence protein intensity level. The IL-4^+ CD4 T cell percentage among total CD4 T cells are quantified below, n=8 mice per group. Three weeks after the first infection, a second infection was given to Great mice (**c,** n=8 mice) or 4get mice (**d,** n=7 mice), bladders and kidneys were collected on Day 1 after the first and second infections for

flow cytometry analysis. WT C57BL/6J mice intravesically infected with UPEC for three days serve as negative control for fluorescence protein intensity level. The quantification of these results is shown (right). The first and second bladder infections were induced in the bladders of C57BL/6J (**e**) or BALB/cJ mice (**f**), then bladders were collected and lysed at the indicated time points. IFN-γ and IL-4 levels in whole bladder lysates were assessed by ELISA and normalized to levels on Day 0, n=6 mice. Black arrows indicate the time point of bacteria delivery. Data are shown as mean ± SD and were analyzed by an unpaired two-tail t test (**a, b**), or an ordinary two-way ANOVA with a Turkey's multiple comparison post-test (**c-f**). *p<0.05, **p<0.01, ***p<0.001, ****p<0.0001, ns= not significant.

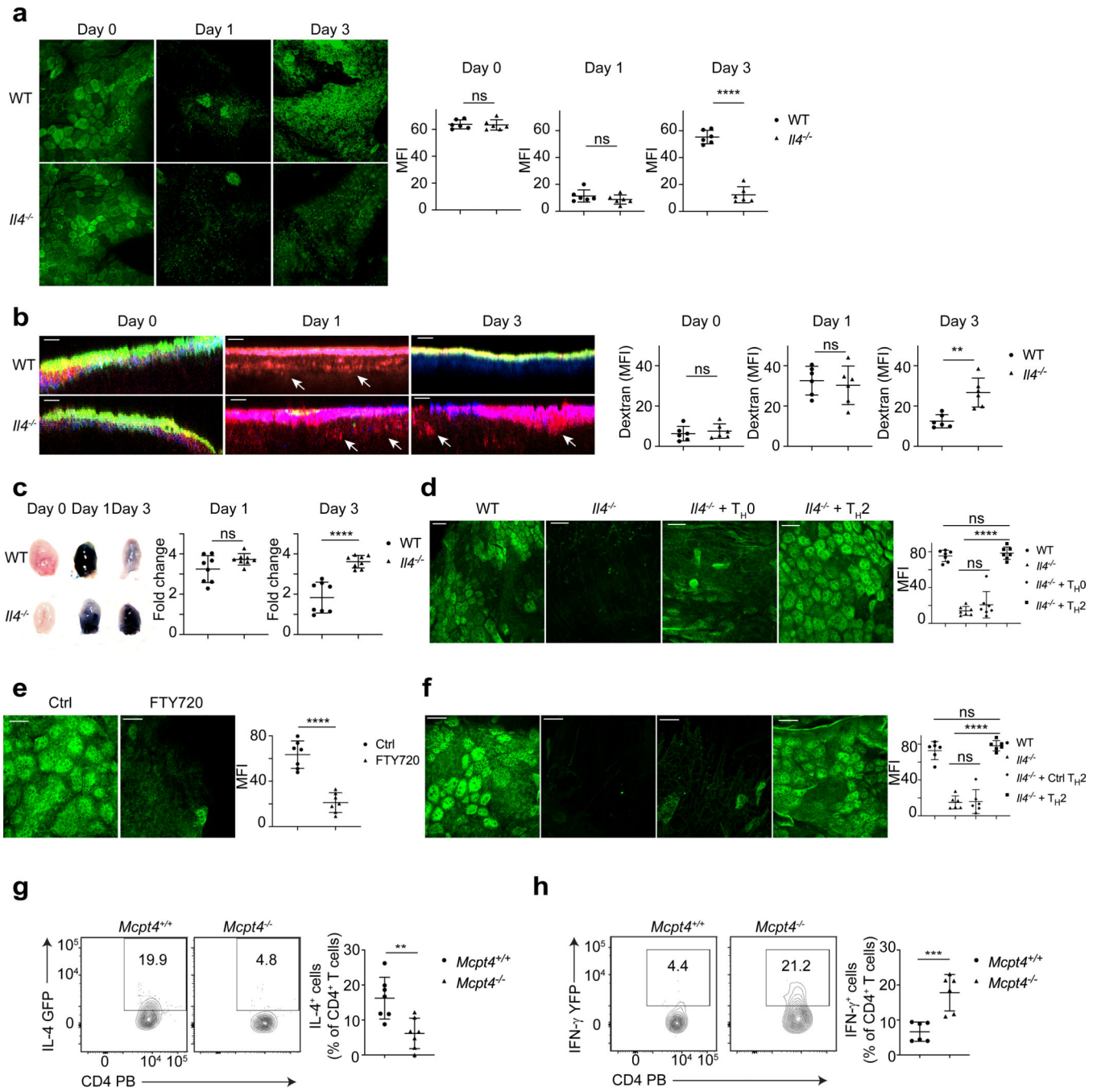

Figure 3. T_H2 cells are necessary for superficial bladder epithelium regeneration.

a, Superficial BECs were labeled by WGA-FITC on Day 0, 1 and 3 after infection. White bar marks 50μm. The mean fluorescence intensity (MFI) of superficial BEC staining was quantified, n=6 mice per group. **b**, On Day 0, 1 and 3 after infection, dextran-Texas Red was applied into the bladder. The pictures showed the sideview of superficial BEC (WGA-FITC, green), general BEC (cytokeratin 5, blue) and dextran (dextran-Texas Red, red). White arrow indicates leaked dextran. White bar depicts 25μm. MFI of dextran-Texas Red underneath BEC was shown (right), n=6 mice. **c**, On Day 0, 1 and 3 after infection, trypan blue staining

of bladder was quantified, n=7 mice. **d**, T_H0 or T_H2 type cells were adoptively transferred into *Il4*$^{-/-}$ mice. The recipient mice were collected for superficial BEC staining on Day 3 after infection. WT and *Il4*$^{-/-}$ mice without transfer served as control. White bar marks 50μm and n=7 mice. **e**, Bladders were collected from FTY720 or dH_2O treated mice for superficial BEC staining on Day 3 after infection. White bar marks 40μm and n=6 mice. **f**, WT, *Il4*$^{-/-}$, *Il4*$^{-/-}$ mice with T_H2 cells from infected 4get and *Il4*$^{-/-}$ mice with control T_H2 cells from culture received bladder infections. Bladders were collected for superficial BEC staining on Day 3 after infection. White bar indicates 50μm and n=6 mice. **g**, Three days after infection, bladders of *Mcpt4*$^{+/+}$ and *Mcpt4*$^{-/-}$ mice were analyzed by flow cytometry. The IL-4$^+$ percentage among total CD4 T cells was quantified, n=6 mice. **h**, IFN-γ$^+$ percentage among total CD4 T cells was quantified, n=6 mice. Data are shown as mean ± SD and were analyzed by an unpaired two-tail t test (**a-c, e, g, h**), or an ordinary one-way ANOVA with a Turkey's multiple comparison post-test (**d, f**). *p< 0.05, **p<0.01, ***p<0.001, ****p<0.0001, ns=not significant.

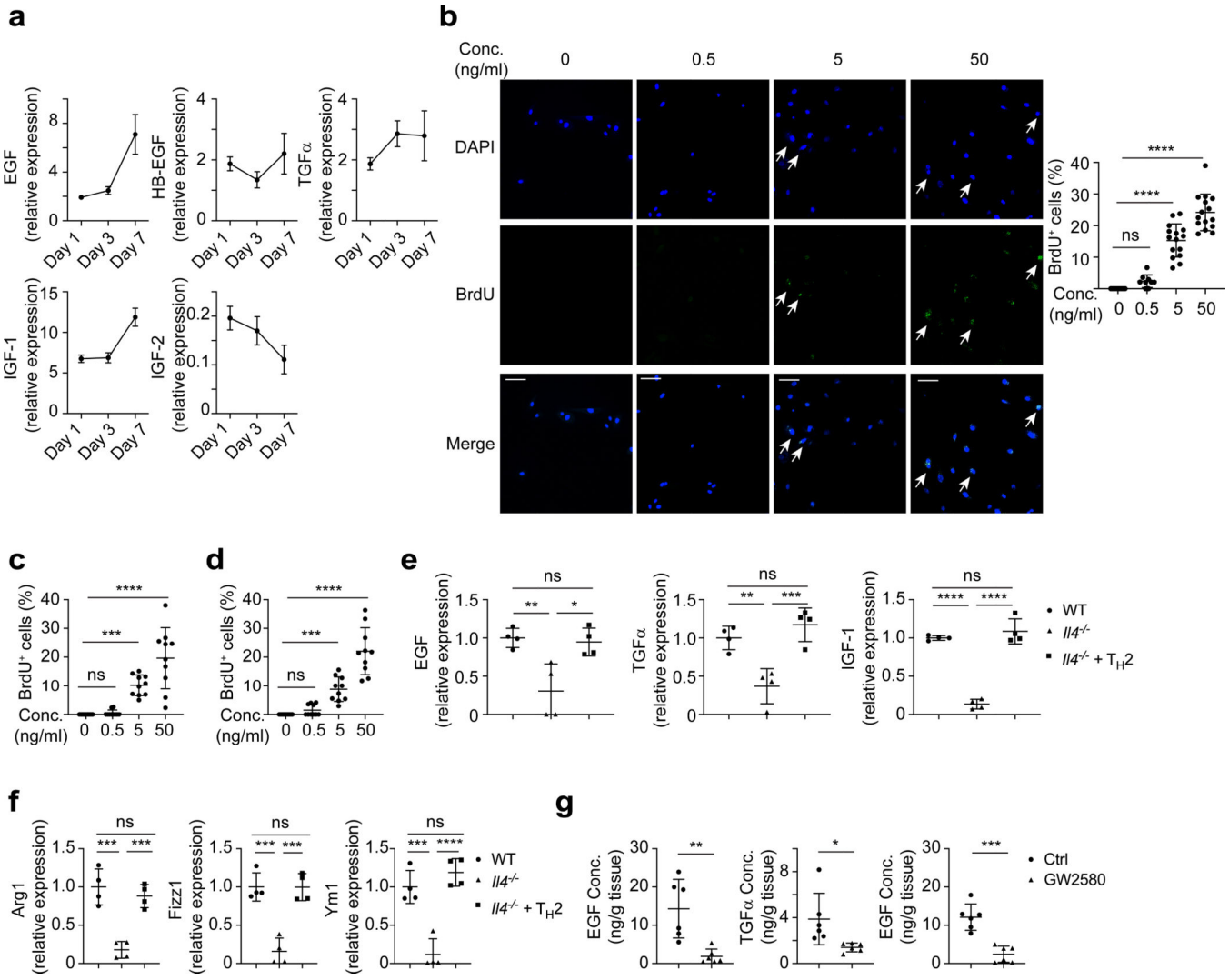

Figure 4. IL-4 regulated growth factors are important for epithelial repair.

a, UPEC was administered into the bladders of WT mice. Bladders were collected on Day 0, 1, 3, and 7 after infection. The level of different growth factor mRNA was assessed by RT-PCR and normalized to levels on Day 0, n=3 mice per time point. **b**, Primary human BECs were co-cultured for 24 hours with BrdU and different concentrations (0, 0.5, 5, 50 ng/ml) of EGF. Cells were stained for BrdU (green) and nuclei (blue). White arrow indicates $BrdU^+$ cells, white bar marks 50μm. The quantification of results is shown (right), n=15 cultures per group. **c**, Culture with TGFα was shown, n=10 cultures. **d**, Culture with IGF-1 was shown, n=10 cultures. **e**, UPEC was used to infect the bladders of WT, *Il4*$^{-/-}$ and *Il4*$^{-/-}$ mice with Th2 transfer. Bladders were collected on Day 3 after infection. The level of different growth factor mRNA was assessed by RT-PCR and normalized to the levels in WT mice, n=4 mice. **f**, The mRNA level of Arg1, Fizz1, and Ym1 of bladders from **e** was assessed by RT-PCR and normalized to the levels in WT mice, n=4 mice. **g**, GW2580 or vehicle control were orally given to WT and the bladders were collected on Day 3 after infection. The concentration of different growth factors in bladder lysate was determined by ELISA, n=6 mice. Data are shown as mean ± SD and were analyzed by an ordinary one-way ANOVA

with a Dunnett's post-test (**b-d**), an ordinary one-way ANOVA with a Turkey's multiple comparison post-test (**e,f**) or an unpaired two-tail t test (**g**). *p<0.05, **p<0.01, ***p<0.001, ****p<0.0001, ns=not significant.

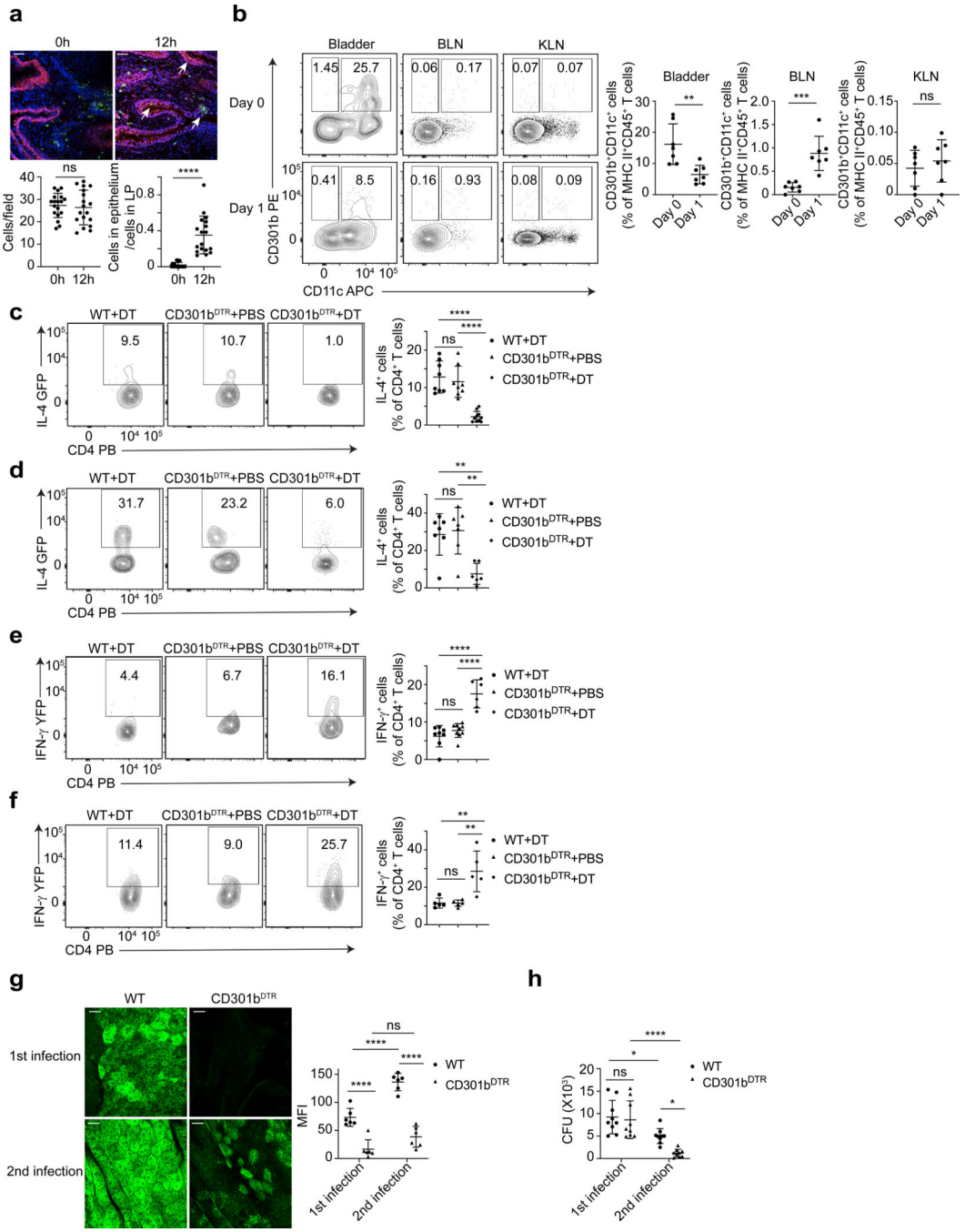

Figure 5. Tissue resident CD301b$^+$ DCs activate T_H2 cells during bladder infection.

a, Bladders were collected at 0h or 12h after infection for staining of CD301b (green), uroepithelium (red) and nuclei (blue). White arrow indicates CD301b+ DC infiltration into epithelium. White bar marks 50 μm. The number of CD301b$^+$ cells per field was counted, the ratio between the number of CD301b$^+$ cells in epithelium and the number of those cells in lamina propria (LP) was determined. n=18 field, and each group has 6 mice. **b**, Samples were collected on Day 0 and Day 1 after infection for flow cytometry analysis. The population shown was pre-gated on 7AAD$^-$CD45$^+$ MHC class II$^+$ single cells and n=7 mice

per group. **c**, Bladders from WT 4get mice with DT, CD301b^{DTR} 4get mice with PBS and CD301b^{DTR} 4get mice with DT were collected on Day 3 after infection for flow cytometry analysis. The quantification of IL-4^{+} percentage was shown, n=8 mice. **d**, Flow cytometry analysis after second infection was shown. n=6 mice. **e**, Bladders from WT Great mice with DT, CD301b^{DTR} Great mice with PBS and CD301b^{DTR} Great mice with DT were collected on Day 3 after infection for flow cytometry analysis. The quantification of IFN-γ^{+} percentage was shown, n=6 mice. **f**, Flow cytometry analysis after second infection was shown, n=5 mice. **g,** Three days after the first or second infection, bladders from WT and CD301b^{DTR} mice were collected for superficial BEC staining. White bar represents 25 μm. MFI of superficial BECs was quantified (right), n=6 mice. **h**, Three days after the first or second infection, bladders from WT and CD301b^{DTR} mice were collected to determine CFU count. Data are shown as mean ± SD and were analyzed by an unpaired two-tail t test (**a,b**), an ordinary one-way (**c-f**) or two-way (**g,h**) ANOVA with a Turkey's multiple comparison post-test. *p<0.05, **p<0.01, ***p<0.001, ****p<0.0001, ns=not significant.

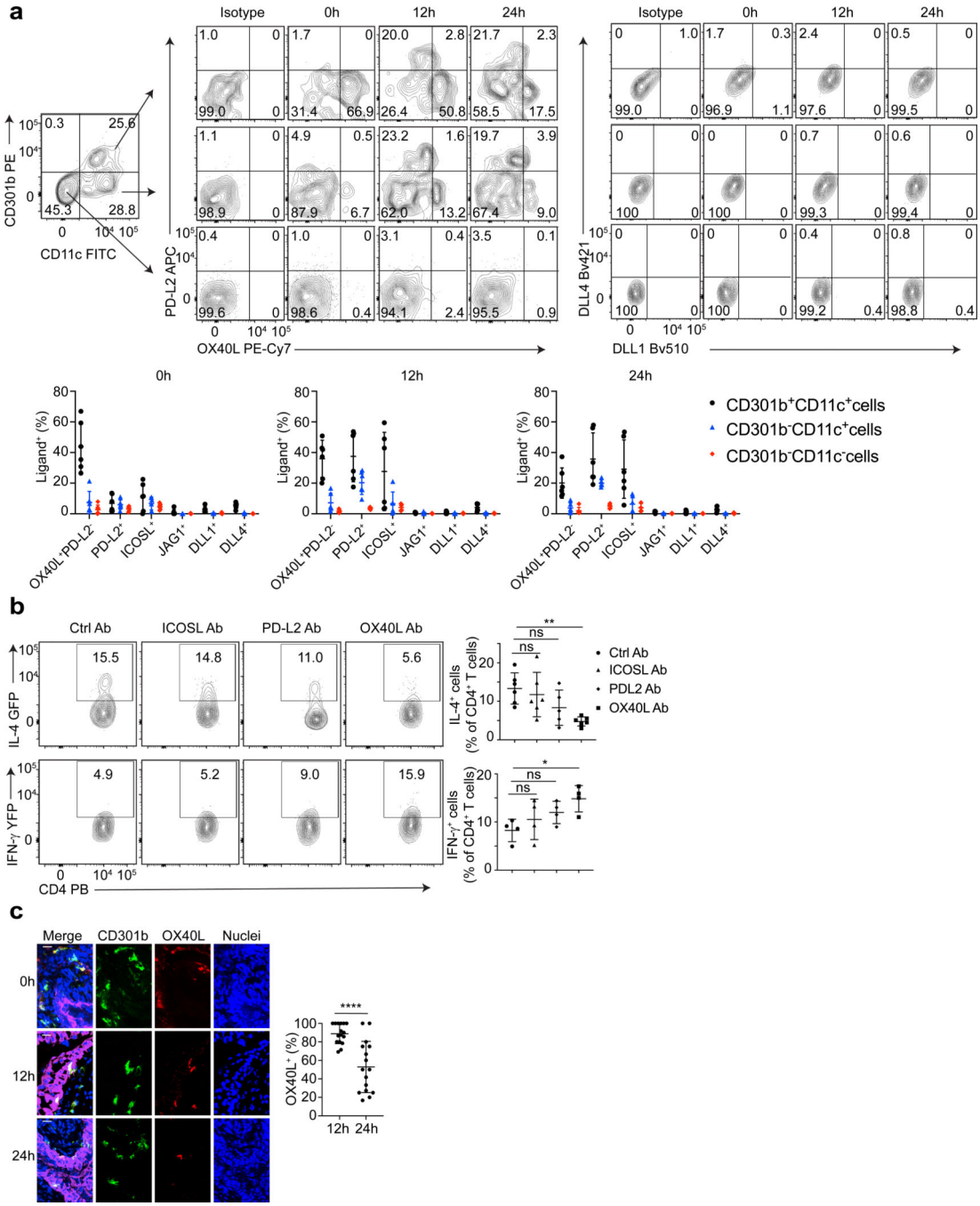

Figure 6. OX40L on CD301b$^+$ DCs is responsible for the induction of T_H2 bias in bladder.

a, Bladders were collected at 0h, 12h, 24h after infection for flow cytometry analysis. The cells were stained for different surface ligands, and cells stained with isotype antibodies served as controls. The quantification results are shown below, in which the percentage of ligand positive cells was shown among the three different APC population for each ligand, n=6 mice. **b**, UPEC was administered to the mice treated with anti-ICOSL Ab, anti-PD-L2 Ab, anti-OX40L Ab or a collection of isotype control antibodies. Three days later, bladders were collected for flow cytometry analysis. The quantification result of IL-4$^+$ (n=6 mice per

group) or IFN-γ^+ (n=4 mice per group) cell percentage among total CD4 T cells was shown in the right. **c**, Bladders were collected at 0h, 12h, 24h after infection for cross section. Samples were stained with nuclei (blue), CD301b (green), OX40L (red), and uroepithelium (magenta). White bar marks 10 μm. The percentage of $OX40L^+CD301b^+$ cells among $CD301b^+$ cells within uroepithelium at 12h and 24h was shown (right). n=16 field, and each group has 4 mice. Data are shown as mean ± SD and were analyzed by an ordinary one-way ANOVA with a Dunnett's post-test comparing each group with a control group (**b**), or an unpaired two-tail t test (**c**). *p<0.05, **p<0.01, ***p<0.001, ****p<0.0001, ns=not significant.

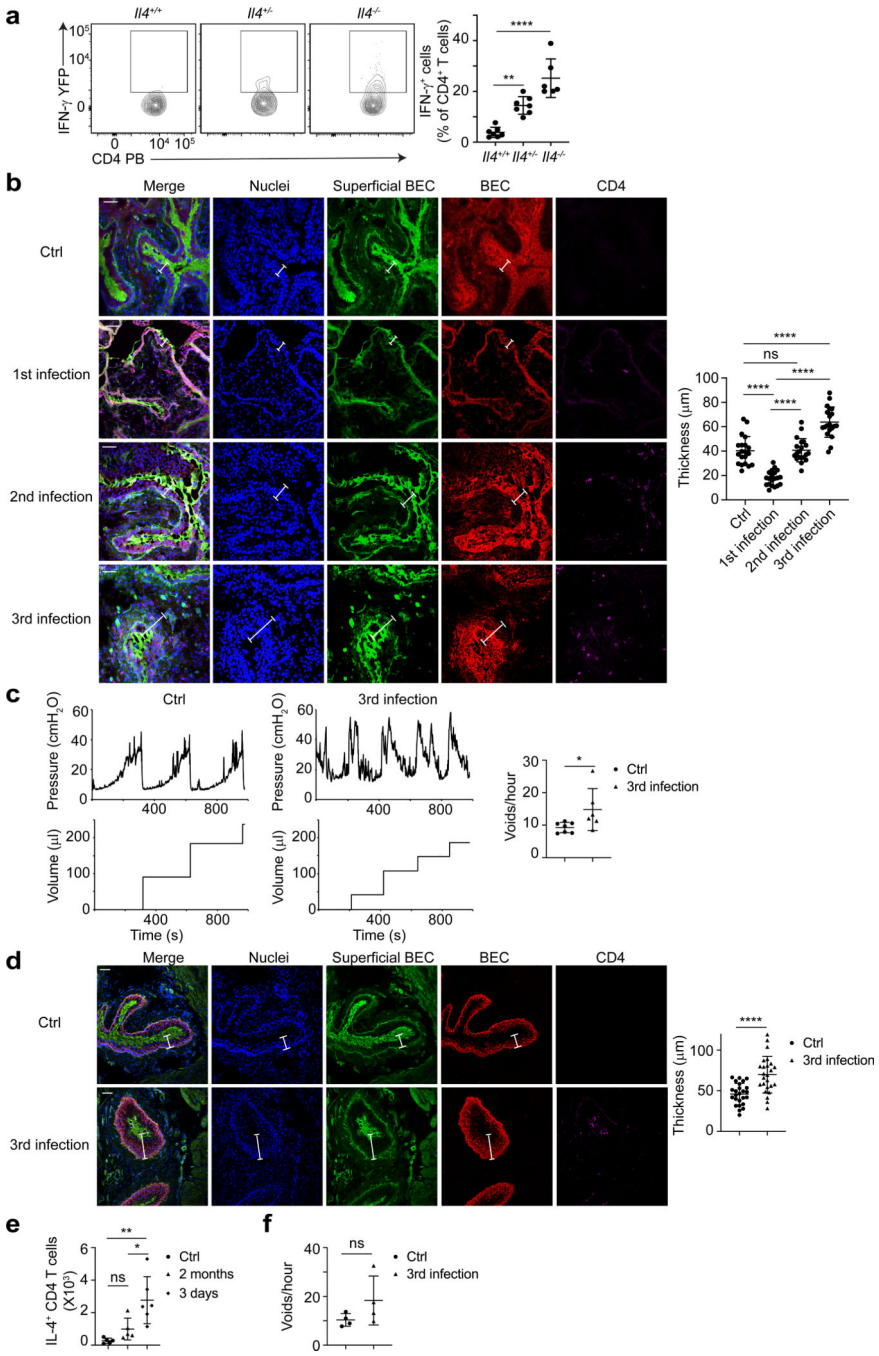

Figure 7. Repeated bladder infections promote T_H2 mediated bladder epithelium repair at the expense of bacterial clearance.

a, UPEC was administered into the bladder of Great mice with *Il4*$^{+/+}$, *Il4*$^{+/-}$ or *Il4*$^{-/-}$. Three days later, bladders were collected for flow cytometry analysis. n=6 mice per group. **b**, Cross section and immunofluorescence staining were done after each infection. Blue is nuclei (DAPI), green is superficial BEC (WGA-FITC), red is total BEC (Cytokeratin 5), magenta is CD4 T cell (CD4). White label indicates the thickness of the epithelium, white bar marks 50μm. Quantification of the epithelium thickness is shown (right), n=4 mice. **c**, Mice

bladders were given three times of UPEC or PBS, and analyzed via bladder cystometry 14 days following the final infection. Representative tracings of intraluminal pressure and void volume are shown (left). The quantitative result of mouse voiding frequency is also shown (right), n=6 mice. **d**, Two months later, bladders were collected for cross section and immune fluorescence staining. Blue is nuclei (DAPI), green is superficial BEC (WGA-FITC), red is total BEC (Cytokeratin 5), magenta is CD4 T cell (CD4). White label indicates the thickness of the epithelium, white bar marks 50μm. Quantification of the epithelium thickness is shown (right), n=5 mice. **e**, IL-4^{+} CD4 T cell number in bladder was determined at 3 days or 2 months after three infections or after PBS treatment. n=6 mice. **f**, Mice bladders were treated three times with UPEC or PBS and analyzed via bladder cystometry two months later. The quantitative result of mouse voiding frequency is shown, n=4 mice. Data are shown as mean ± SD and were analyzed by an ordinary one-way ANOVA with a Turkey's multiple comparison post-test (**a, b, e**), or an unpaired two-tail t test (**c, d, f**). *p<0.05, **p<0.01, ***p<0.001, ****p<0.0001, ns=not significant.